


Solution generation of a capped black hole

Ryotaku Suzuki^{*} and Shinya Tomizawa[†]

*Mathematical Physics Laboratory, Toyota Technological Institute
Hisakata 2-12-1, Tempaku-ku, Nagoya 468-8511, Japan*

 (Received 30 April 2024; accepted 17 May 2024; published 12 July 2024)

Utilizing the electric Harrison transformation developed in five-dimensional minimal supergravity, we construct an exact solution characterizing non-BPS (Bogomol'nyi-Prasad-Sommerfield) charged rotating black holes with a horizon cross section of a lens space $L(n; 1)$. Among these solutions, only the ones corresponding to $n = 0$ and $n = 1$ do not have any curvature singularities, conical singularities, Dirac-Misner string singularities, and orbifold singularities both on and outside the horizon; additionally, they are free from closed timelike curves. The solution for $n = 0$ corresponds to the charged dipole black ring that we constructed in the previous paper. The specific solution for $n = 1$, referred to as the “capped black hole,” was introduced in our previous article. This provides the first example of a non-BPS exact solution, representing an asymptotically flat, stationary spherical black hole with a domain of outer communication (DOC) having a nontrivial topology in five-dimensional minimal supergravity. We demonstrate that the DOC on a time slice has the topology of $[\mathbb{R}^4 \# \mathbb{C}P^2] \setminus \mathbb{B}^4$. Differing from the well-known Myers-Perry and Cvetič-Youm black holes describing a spherical horizon topology and a DOC with a trivial topology of $\mathbb{R}^4 \setminus \mathbb{B}^4$ on a timeslice, the capped black hole’s horizon is capped by a disk-shaped bubble. We explicitly demonstrate that the capped black hole carries mass, two angular momenta, an electric charge, and a magnetic flux, with only three of these quantities being independent. Furthermore, we reveal that this black hole can possess identical conserved charges as the Cvetič-Youm black hole. The existence of this solution challenges black hole uniqueness beyond both the black ring and the BPS spherical black hole. Moreover, within specific parameter regions, the capped black hole can exhibit larger entropy than the Cvetič-Youm black hole.

DOI: [10.1103/PhysRevD.110.024026](https://doi.org/10.1103/PhysRevD.110.024026)

I. INTRODUCTION

In the domain of string theory and its associated disciplines, higher-dimensional black holes and other extended black objects have played a pivotal role in our comprehension of these higher-dimensional theories over the past two decades [1,2]. Of particular interest is the physics of black holes within the framework of five-dimensional minimal supergravity, which is recognized as a low-energy approximation of string theory. This theory shares similarities with eleven-dimensional supergravity, particularly in terms of its Lagrangians, where the three-form field in eleven-dimensional supergravity is replaced by Maxwell’s $U(1)$ gauge field. The correspondence between five-dimensional minimal supergravity and eleven-dimensional supergravity has been previously

investigated [3,4]. Furthermore, the formulation of five-dimensional supergravity can be derived through a truncated toroidal compactification of eleven-dimensional supergravity by identifying three vector fields and freezing out the moduli [5,6]. This highlights the significance of discovering and classifying all exact solutions of black holes within the framework of five-dimensional minimal supergravity, as it contributes significantly to our understanding of string theory. Despite ongoing efforts, achieving this goal remains elusive, although various exact solutions of black holes within this theory have been generated through recent advancements in solution-generation techniques [7–14].

It is now well-established that even within vacuum Einstein gravity, there exists a diverse kind of black hole solutions in higher dimensions [15,16]. However, the classification of asymptotically flat and stationary black holes remains a significant open problem. For instance, according to the topology theorem of a stationary black hole in five dimensions [17], the allowed topology of the cross section of the event horizon is restricted to either a sphere S^3 , a ring $S^1 \times S^2$, or lens spaces $L(n; m)$, given the spacetime is asymptotically flat and allows two commuting axial Killing vector fields. Emparan and Reall [16] first

^{*}sryotaku@toyota-ti.ac.jp

[†]tomizawa@toyota-ti.ac.jp

Published by the American Physical Society under the terms of the Creative Commons Attribution 4.0 International license. Further distribution of this work must maintain attribution to the author(s) and the published article’s title, journal citation, and DOI. Funded by SCOAP³.

showed that five-dimensional vacuum Einstein theory allows for the existence of a S^1 -rotating spherical black hole and two rotating black rings with identical conserved charges, thus explicitly illustrating the nonuniqueness property in higher dimensions. The S^2 -rotating black ring was initially derived independently by Mishima and Iguchi [18] and Figueras [19], although it exhibited conical singularities. Subsequently, Pomerasnky and Sen'kov [20] succeeded in constructing the general black ring solution with rotations in both S^1 and S^2 . Numerous efforts have been made by various authors to discover an asymptotically flat black lens solution to the five-dimensional vacuum Einstein equations. However, regrettably, all such endeavors have ended in failure [21–24]. The main obstacle lies in the fact that the resulting solutions obtained are always marred by naked singularities. Several black objects have been extensively studied within the context of asymptotically flat supersymmetric solutions in five-dimensional minimal supergravity, leveraging techniques pioneered by Gauntlett *et al.* [25]. Reall demonstrated that the possible topologies of these supersymmetric black holes are limited to S^3 , $S^1 \times S^2$, T^3 , or quotients thereof [26]. For the S^3 case, Breckenridge *et al.* [27] constructed a black hole solution with spherical topology featuring equal angular momenta, commonly referred to as the Breckenridge-Myers-Peet-Vafa (BMPV) black hole. Elvang *et al.* discovered a black ring solution in the $S^1 \times S^2$ case [28]. The black ring exhibits only $U(1) \times U(1)$ spatial symmetry and does not allow for a configuration with equal angular momenta, distinguishing it from the BMPV black hole. Furthermore, Kunduri and Lucietti constructed an asymptotically flat supersymmetric black lens solution with topology $L(2; 1) = S^3/\mathbb{Z}_2$ [29], which was later extended to more general black lens solutions with topology $L(n; 1) = S^3/\mathbb{Z}_n$ ($n \geq 3$) in Refs. [30,31]. So far, exact solutions for biaxially symmetric Bogomol'nyi-Prasad-Sommerfield (BPS) black holes have been classified [31], but ones for non-BPS black holes with a single $U(1)$ symmetry, or even $U(1) \times U(1)$, remain elusive.

In recent years, many researchers have focused on horizon topologies when constructing new exact solutions of black holes. However, it has recently become evident that different types of black holes can exist even when the horizon topology is spherical. According to the uniqueness theorem for charged rotating black holes in the bosonic sector of five-dimensional minimal supergravity [32], assuming the existence of two commuting axial isometries and a spherical topology of horizon cross sections, an asymptotically flat, stationary charged rotating black hole with a nonextremal horizon is uniquely characterized by its mass, charge, and two independent angular momenta, and is therefore described by the five-dimensional Cvetic-Youm solution [33]. Consequently, it appears that there are no other spherical black holes in the class of asymptotically flat, regular solutions with no closed timelike curves (CTCs).

However, the topological censorship theorem proved by Friedman [34] gives the possibility of another black hole with spherical topology since in the uniqueness theorem [32], the exterior region of a black hole is assumed to have the trivial topology of $\mathbb{R}^4 \setminus \mathbb{B}^4$, where \mathbb{B}^4 represents the black hole region. This theorem asserts that under the averaged null energy condition, the domain of outer communication (DOC) in an asymptotically flat spacetime must be simply connected. In four dimensions, this implies that the topology of the intersection of a black hole's exterior region with a time slice Σ is limited to a trivial structure of $\mathbb{R}^3 \setminus \mathbb{B}^3$, where \mathbb{B}^3 represents the black hole region. However, in higher dimensions, the DOC can exhibit nontrivial topologies, meaning that $\text{DOC} \cap \Sigma$ can possess homology groups with ranks higher than one. Based on the topological censorship theorem, it was shown in Ref. [35] that in five dimensions, the region $\text{DOC} \cap \Sigma$ can have the nontrivial topology of $[\mathbb{R}^4 \# n(S^2 \times S^2) \# m(\pm \mathbb{C}\mathbb{P}^2)] \setminus \mathbb{B}^4$. In static asymptotically flat spacetimes, the uniqueness theorems [36,37] establish that the higher-dimensional Schwarzschild and Reissner-Nordström solutions [38] are the only vacuum and charged black hole solutions, respectively. Consequently, any solutions with a nontrivial DOC—if they exist—must belong to a class of solutions that are not static rather stationary. Kunduri and Lucietti [39] have constructed a four parameter family of supersymmetric black hole solutions with spherical horizon topology and two two-cycles in the exterior in five-dimensional minimal supergravity, which indicates a charged spherical black hole such that $\text{DOC} \cap \Sigma$ has the topology of $[\mathbb{R}^4 \# S^2 \times S^2] \setminus \mathbb{B}^4$. The presence of such a solution indicates the existence of black holes within this family that possess conserved charges identical to those of the BMPV black hole [27], highlighting the violation of uniqueness among black holes within a certain class of BPS spherical black holes.

It is well known that dimensionally reduced gravity theories and supergravity exhibit a global symmetry known as “hidden symmetry,” which often proves to be a powerful tool in discovering new solutions. New solutions can be obtained by applying this group transformation to a known solution within the same theory, referred to as a “seed solution” (see Refs. [40–42] for four-dimensional Einstein gravity). The dimensional reduction of five-dimensional minimal supergravity to four dimensions, as explored in Refs. [3,43], reveals precisely an $SL(2, \mathbb{R})$ symmetry, arising from the dimensional reduction of eleven-dimensional supergravity [44]. The new solution-generation technique utilizing this $SL(2, \mathbb{R})$ symmetry [13] has successfully produced the Kaluza-Klein black hole solutions [45,46]. First explored by Mizoguchi and Ohta [3,4] in five-dimensional minimal supergravity, the presence of two commuting Killing vector fields reduces the theory to a three-dimensional nonlinear sigma model with a $G_{2(2)}$ target space symmetry. With two spacelike commuting

Killing vector fields, it is described by the $G_{2(2)}/SO(4)$ sigma model coupled to gravity, while if one of the two commuting Killing vector fields is timelike, the symmetry becomes $G_{2(2)}/[SL(2, \mathbb{R}) \times SL(2, \mathbb{R})]$. Utilizing this $G_{2(2)}$ symmetry, Bouchareb *et al.* [14] developed a solution-generation technique involving an electric Harrison transformation, capable of transforming a five-dimensional vacuum solution into an electrically charged solution in five-dimensional minimal supergravity. By representing the coset in terms of a 7×7 matrix, this transformation applied to the five-dimensional vacuum rotating black hole (the Myers-Perry solution [15]) yields the five-dimensional charged rotating black hole (the Cvetič-Youm solution [33]). However, applying this transformation to the vacuum doubly rotating black ring (the Pomeransky-Sen'kov solution [20]) fails to produce a regular charged doubly spinning black ring solution, as the resulting solution inevitably suffers from a Dirac-Misner string singularity. In Ref. [47], this transformation is also applied to the Rasheed solution [48] producing the rotating generalization of the static charged Kaluza-Klein black hole found by Ishihara and Matsuno [49].

In our prior research [50], we employed the electric Harrison transformation to derive an exact solution for a non-BPS charged rotating black ring with a dipole charge within the bosonic sector of five-dimensional minimal supergravity. To achieve this solution, we employed a vacuum solution of a rotating black ring that inherently contained a Dirac-Misner string singularity as the seed solution for the Harrison transformation. Subsequently, we adjusted the parameters appropriately to eliminate the Dirac-Misner string singularity inside the black ring. To procure a vacuum seed solution having a Dirac-Misner string singularity, the inverse scattering method (ISM) proves invaluable. In Ref. [50], we successfully constructed such a vacuum solution, which serves as the foundational seed for the Harrison transformation. The ISM stands out as one of the most valuable tools for obtaining exact solutions of the vacuum Einstein equations with $D - 2$ Killing isometries (D : spacetime dimension). This method enables the systematic derivation of new solutions with the same isometries through the soliton transformation from a known simple solution. While the original ISM, as formulated by Belinski and Zakharov [51,52], typically yields singular solutions when applied directly to higher dimensions, Pomeransky modified the ISM to generate regular solutions even in higher dimensions [53]. Notably, when combined with the rod structure [54,55], this modified ISM has been highly successful, particularly in the context of five-dimensional vacuum black hole solutions [12,18,20–24,56–79]. The first example of this success was the rederivation of the five-dimensional Myers-Perry black hole solution [53]. Subsequently, the S^2 -rotating black ring was rederived from the Minkowski seed [58], though the generation of the S^1 -rotating black ring presented a more delicate

problem due to the choice of seed leading to singular solutions. The appropriate seed for deriving the black ring with S^1 rotation was first considered in [56,57], culminating in the construction of the regular black ring solution with both S^1 and S^2 rotations by Pomeransky and Sen'kov [20]. In attempts to construct asymptotically flat black lens solutions in five-dimensional Einstein equations, several authors have employed the ISM. For instance, Evslin [21] attempted to construct a static black lens with lens space topology $L(n^2 + 1; 1)$, only to find that while orbifold singularities could be eliminated, curvature singularities remained unavoidable. Similarly, Chen and Teo [22] constructed a black lens solution with horizon topology $L(n; 1) = S^3/\mathbb{Z}_n$ by the ISM, but encountered either conical singularities or naked curvature singularities. The primary obstacle in constructing black lens solutions has thus been the presence of naked singularities. However, breakthroughs in this regard have emerged from supersymmetric solutions [29–31].

In this paper, we derive an exact solution representing an asymptotically flat, stationary, non-BPS black hole characterized by a horizon cross section with trivial topology S^3 and a DOC exhibiting nontrivial topology, within the bosonic sector of five-dimensional minimal supergravity. To begin, we employ the ISM to construct a vacuum black lens harboring a Dirac-Misner string singularity. Subsequently, employing the electric Harrison transformation on this vacuum solution, we derive a charged rotating black lens solution characterized by a horizon topology of lens space $L(n; 1)$, still retaining the Dirac-Misner string singularity. Finally, we adjust the solution's parameters to eliminate the Dirac-Misner string singularity, ensuring its regularity. Among these solutions, only those corresponding to $n = 0$ and $n = 1$ exhibit regularity, the absence of curvature, conical, Dirac-Misner string, or orbifold singularities both inside and outside the horizon, and additionally CTCs. The $n = 0$ solution corresponds to the charged dipole black ring previously constructed in our earlier work [50]. Specifically, the $n = 1$ solution, termed the ‘‘capped black hole,’’ was introduced in our preceding work [79]. This presents the first instance of a non-BPS exact solution, delineating an asymptotically flat, stationary spherical black hole with a nontrivially topological DOC within five-dimensional minimal supergravity. In contrast to the familiar Cvetič-Youm solution with a spherical horizon topology, the capped black hole's horizon is capped by a disk-shaped bubble. Additionally, we demonstrate the existence of spherical black holes possessing the same conserved charges as the Cvetič-Youm solution, which implies the violation of the uniqueness for a spherical black hole.

The remainder of this paper is structured as follows: In Sec. II, we provide an overview of the setup and formalism employed in our analysis. Section III is dedicated to the construction of the neutral metric using the soliton

transformation. Following this, in Sec. IV, we detail the application of the electric Harrison transformation to the neutral metric, resulting in the derivation of the charged metric and gauge field. Furthermore, we demonstrate that the only regular charged solution corresponds to a black ring and a black hole with a disklike bubble. Subsequently, in Sec. V, we delve into an examination of the physical properties of the regular black hole solution. Finally, we encapsulate our findings and conclusions in Sec. VI.

II. PRELIMINARY

Let us start by explaining the fundamental framework for asymptotically flat, stationary, and biaxially symmetric solutions within the bosonic sector of five-dimensional minimal ungauged supergravity (Einstein-Maxwell-Chern-Simons theory). The action governing this theory is given by

$$S = \frac{1}{16\pi G_5} \left[\int d^5x \sqrt{-g} \left(R - \frac{1}{4} F^2 \right) - \frac{1}{3\sqrt{3}} \int F \wedge F \wedge A \right], \quad (1)$$

where $F = dA$. The field equations governing the dynamics of the system consist of the Einstein equation and the Maxwell equation with a Chern-Simons term. They are expressed as

$$R_{\mu\nu} - \frac{1}{2} R g_{\mu\nu} = \frac{1}{2} \left(F_{\mu\lambda} F_{\nu}{}^{\lambda} - \frac{1}{4} g_{\mu\nu} F_{\rho\sigma} F^{\rho\sigma} \right), \quad (2)$$

and

$$d\star F + \frac{1}{\sqrt{3}} F \wedge F = 0. \quad (3)$$

A. Five-dimensional minimal supergravity with symmetry

By assuming the presence of one timelike Killing vector $\xi_0 = \partial/\partial t$ and one spacelike axial Killing vector $\xi_1 = \partial/\partial\psi$, the theory reduces to the $G_{2(2)}/SL(2, \mathbb{R}) \times SL(2, \mathbb{R})$ nonlinear sigma models coupled to three-dimensional gravity [3,4]. Further, the assumption of the existence of a third spacelike axial Killing vector $\xi_2 = \partial/\partial\phi$, implying the presence of three mutually commuting Killing vectors, reduces the theory to a two-dimensional nonlinear sigma model, and additionally ensures the integrability conditions discussed in Ref. [54,55]; as a result, the metric can be expressed in the Weyl-Papapetrou form:

$$ds^2 = \lambda_{ab} (dx^a + a^a{}_{\phi} d\phi) (dx^b + a^b{}_{\phi} d\phi) + \tau^{-1} \rho^2 d\phi^2 + \tau^{-1} e^{2\sigma} (d\rho^2 + dz^2), \quad (4)$$

and the gauge potential is given by

$$A = \sqrt{3} \psi_a dx^a + A_{\phi} d\phi, \quad (5)$$

where the coordinates $x^a = (t, \psi)$ ($a = 0, 1$) represent the Killing coordinates, and thus all functions λ_{ab} , $\tau := -\det(\lambda_{ab})$, a^a , σ , and (ψ_a, A_{ϕ}) are independent of ϕ and x^a . Additionally, as shown in the Appendix of Ref. [32], one can always set $A_{\rho} = A_z = 0$, using the gauge transformation. It is important to note that the coordinates (ρ, z) , spanning a two-dimensional base space $\Sigma = \{(\rho, z) | \rho \geq 0, -\infty < z < \infty\}$, are globally well defined, harmonic, and mutually conjugate on Σ .

The magnetic potential μ and twist potentials ω_a can be introduced using Eqs. (2) and (3), as discussed in Ref. [32], expressed as

$$d\mu = \frac{1}{\sqrt{3}} \star (\xi_0 \wedge \xi_1 \wedge F) - \epsilon^{ab} \psi_a d\psi_b, \quad (6)$$

$$d\omega_a = \star (\xi_0 \wedge \xi_1 \wedge d\xi_a) + \psi_a (3d\mu + \epsilon^{bc} \psi_b d\psi_c), \quad (7)$$

where $\epsilon^{01} = -\epsilon^{10} = 1$, and ξ_a ($a = 0, 1$) are written as Killing one-forms. Thus, as a consequence of the existence of isometries ξ_a , we have eight scalar fields $\lambda_{ab}, \omega_a, \psi_a, \mu$, which we denote collectively by coordinates $\Phi^A = (\lambda_{ab}, \omega_a, \psi_a, \mu)$ ($a = 0, 1$) and then, the action (1) reduces to the following nonlinear sigma model for the eight scalar functions Φ^A invariant under the $G_{2(2)}$ transformation:

$$S = \int d\rho dz \rho [G_{AB} (\partial\Phi^A) (\partial\Phi^B)] = \int d\rho dz \rho \left[\frac{1}{4} \text{Tr}(\lambda^{-1} \partial\lambda \lambda^{-1} \partial\lambda) + \frac{1}{4} \tau^{-2} \partial\tau^2 + \frac{3}{2} \partial\psi^T \lambda^{-1} \partial\psi - \frac{1}{2} \tau^{-1} v^T \lambda^{-1} v - \frac{3}{2} \tau^{-1} (\partial\mu + \epsilon^{ab} \psi_a \partial\psi_b)^2 \right], \quad (8)$$

where $v = \partial\omega - \psi(3d\mu + \epsilon^{bc} \psi_b \partial\psi_c)$. In this coordinate system, $\Phi^A = (\lambda_{ab}, \omega_a, \psi_a, \mu)$ are determined by the equations of motion

$$\Delta_{\gamma} \Phi^A + \Gamma_{BC}^A [\Phi_{,\rho}^B \Phi_{,\rho}^C + \Phi_{,z}^C \Phi_{,z}^C] = 0, \quad (9)$$

where Δ_{γ} is the Laplacian with respect to the abstract three-dimensional metric $\gamma = d\rho^2 + dz^2 + \rho^2 d\phi^2$, and Γ_{BC}^A is the Christoffel symbol with respect to the target space metric G_{AB} .

On the other hand, once Φ^A are given, one can completely determine σ , $a^t{}_{\phi}$, $a^{\psi}{}_{\phi}$, A_i . In fact, the function σ is determined by

$$\frac{2}{\rho} \sigma_{,\rho} = G_{AB} [\Phi_{,\rho}^A \Phi_{,\rho}^B - \Phi_{,z}^A \Phi_{,z}^B], \quad \frac{1}{\rho} \sigma_{,z} = G_{AB} \Phi_{,\rho}^A \Phi_{,z}^B. \quad (10)$$

The integrability $\sigma_{,\rho z} = \sigma_{,z\rho}$ is assured by Eq. (9). From Eq. (7), the metric functions a^a_{ϕ} are determined by

$$\begin{aligned} a^a_{\phi,\rho} &= -\rho\tau^{-1}\lambda^{ab}(\omega_{b,z} - 3\psi_b\mu_{,z} - \psi_b\epsilon^{cd}\psi_c\psi_{d,z}), \\ a^a_{\phi,z} &= \rho\tau^{-1}\lambda^{ab}(\omega_{b,\rho} - 3\psi_b\mu_{,\rho} - \psi_b\epsilon^{cd}\psi_c\psi_{d,\rho}), \end{aligned} \quad (11)$$

where we have set

$$\epsilon_{012\rho z} = 1. \quad (12)$$

Therefore it follows from Eq. (6) that the gauge potential A_ϕ is determined by

$$A_{\phi,\rho} = \sqrt{3}[a^a_{\phi}\psi_{a,\rho} - \rho\tau^{-1}(\mu_{,z} + \epsilon^{bc}\psi_b\psi_{c,z})], \quad (13)$$

$$A_{\phi,z} = \sqrt{3}[a^a_{\phi}\psi_{a,z} + \rho\tau^{-1}(\mu_{,\rho} + \epsilon^{bc}\psi_b\psi_{c,\rho})]. \quad (14)$$

Thus, once $\Phi^A = (\lambda_{ab}, \omega_a, \psi_a, \mu)$ are determined, one can determine the solutions of the system given by the action (1).

Following Ref. [14], we introduce the $G_{2(2)}/[SL(2, R) \times SL(2, R)]$ coset matrix, M , which is defined by

$$M = \begin{pmatrix} \hat{A} & \hat{B} & \sqrt{2}\hat{U} \\ \hat{B}^T & \hat{C} & \sqrt{2}\hat{V} \\ \sqrt{2}\hat{U}^T & \sqrt{2}\hat{V}^T & \hat{S} \end{pmatrix}, \quad (15)$$

where \hat{A} and \hat{C} are symmetric 3×3 matrices, \hat{B} is a 3×3 matrix, \hat{U} and \hat{V} are three-component column matrices, and \hat{S} is a scalar, defined, respectively, by

$$\begin{aligned} \hat{A} &= \begin{pmatrix} [(1-y)\lambda + (2+x)\psi\psi^T - \tau^{-1}\tilde{\omega}\tilde{\omega}^T + \mu(\psi\psi^T\lambda^{-1}\hat{J} - \hat{J}\lambda^{-1}\psi\psi^T)] & \tau^{-1}\tilde{\omega} \\ \tau^{-1}\tilde{\omega}^T & -\tau^{-1} \end{pmatrix}, \\ \hat{B} &= \begin{pmatrix} (\psi\psi^T - \mu\hat{J})\lambda^{-1} - \tau^{-1}\tilde{\omega}\psi^T\hat{J} & [-(1+y)\lambda\hat{J} - (2+x)\mu + \psi^T\lambda^{-1}\tilde{\omega}]\psi + (z - \mu\hat{J}\lambda^{-1})\tilde{\omega} \\ \tau^{-1}\psi^T\hat{J} & -z \end{pmatrix}, \\ \hat{C} &= \begin{pmatrix} (1+x)\lambda^{-1} - \lambda^{-1}\psi\psi^T\lambda^{-1} & \lambda^{-1}\tilde{\omega} - \hat{J}(z - \mu\hat{J}\lambda^{-1})\psi \\ \tilde{\omega}^T\lambda^{-1} + \psi^T(z + \mu\lambda^{-1}\hat{J})\hat{J} & [\tilde{\omega}^T\lambda^{-1}\tilde{\omega} - 2\mu\psi^T\lambda^{-1}\tilde{\omega} - \tau(1+x-2y-xy+z^2)] \end{pmatrix}, \\ \hat{U} &= \begin{pmatrix} (1+x - \mu\hat{J}\lambda^{-1})\psi - \mu\tau^{-1}\tilde{\omega} \\ \mu\tau^{-1} \end{pmatrix}, \\ \hat{V} &= \begin{pmatrix} (\lambda^{-1} + \mu\tau^{-1}\hat{J})\psi \\ \psi^T\lambda^{-1}\tilde{\omega} - \mu(1+x-z) \end{pmatrix}, \\ \hat{S} &= 1 + 2(x-y), \end{aligned}$$

with

$$\tilde{\omega} = \omega - \mu\psi, \quad (16)$$

$$x = \psi^T\lambda^{-1}\psi, \quad y = \tau^{-1}\mu^2, \quad z = y - \tau^{-1}\psi^T\hat{J}\tilde{\omega}, \quad (17)$$

and the 2×2 matrix,

$$\hat{J} = \begin{pmatrix} 0 & 1 \\ -1 & 0 \end{pmatrix}. \quad (18)$$

We note that this 7×7 matrix M is symmetric, $M^T = M$, and unimodular, $\det(M) = 1$. We define a current matrix as

$$J_i = M^{-1}\partial_i M, \quad (19)$$

which is conserved if the scalar fields are the solutions of the equation of motion derived by the action (8). Then, the action (8) can be written in terms of J or M as follows:

$$\begin{aligned} S &= \frac{1}{4} \int d\rho dz \rho \text{tr}(J_i J^i) \\ &= \frac{1}{4} \int d\rho dz \rho \text{tr}(M^{-1}\partial_i M M^{-1}\partial^i M). \end{aligned} \quad (20)$$

Thus, the matrix M completely specifies the solutions to our system. In terms of this, one can find that the equation of motion (9) can be written as

$$\partial_\rho(\rho\partial_\rho M M^{-1}) + \partial_z(\rho\partial_z M M^{-1}) = 0. \quad (21)$$

The action (20) is invariant under the $G_{2(2)}$ transformation.

B. Electric Harrison transformation

In particular, utilizing the $G_{2(2)}$ symmetry, Ref. [14] constructed the electric Harrison transformation preserving asymptotic flatness that transforms a five-dimensional

vacuum solution $\Phi^A = \{\lambda_{ab}, \omega_a, \psi_a = 0, \mu = 0\}$ into a charged solution $\Phi'^A = \{\lambda'_{ab}, \omega'_a, \psi'_a, \mu'\}$ in five-dimensional minimal supergravity, which is given by

$$\begin{aligned} \tau' &= D^{-1}\tau, & \lambda'_{00} &= D^{-2}\lambda_{00}, & \lambda'_{01} &= D^{-2}(c^3\lambda_{01} + s^3\lambda_{00}\omega_0), \\ \lambda'_{11} &= -\frac{\tau D}{\lambda_{00}} + \frac{(c^3\lambda_{01} + s^3\omega_0\lambda_{00})^2}{D^2\lambda_{00}}, \\ \omega'_0 &= D^{-2}[c^3(c^2 + s^2 + 2s^2\lambda_{00})\omega_0 - s^3(2c^2 + (c^2 + s^2)\lambda_{00})\lambda_{01}], \\ \omega'_1 &= \omega_1 + D^{-2}s^3[-c^3\lambda_{01}^2 + s(2c^2 - \lambda_{00})\lambda_{01}\omega_0 - c^3\omega_0^2], \\ \psi'_0 &= D^{-1}sc(1 + \lambda_{00}), & \psi'_1 &= D^{-1}sc(c\lambda_{01} - s\omega_0), \\ \mu' &= D^{-1}sc(c\omega_0 - s\lambda_{01}), \end{aligned} \quad (22)$$

with

$$D = c^2 + s^2\lambda_{00} = 1 + s^2(1 + \lambda_{00}), \quad (23)$$

where the new parameter α in $(c, s) := (\cosh \alpha, \sinh \alpha)$ is related to the electric charge. The functions a^a_ϕ ($a = 0, 1$) and the component A'_ϕ for the charged solution are determined by the eight scalar functions $\{\lambda'_{ab}, \omega'_a, \psi'_a, \mu'\}$ from Eqs. (6) and (7) after the replacement of $\{\lambda_{ab}, \omega_a, \psi_a, \mu\}$ with $\{\lambda'_{ab}, \omega'_a, \psi'_a, \mu'\}$: First, the functions a^a_ϕ ($a = 0, 1$) are determined by

$$\begin{aligned} \partial_\rho a^a_\phi &= -\frac{\rho}{\tau} \lambda'^{ab} (\partial_z \omega'_b - 3\psi'_b \partial_z \mu' - \psi'_b \epsilon^{cd} \psi'_c \partial_z \psi'_d), \\ \partial_z a^a_\phi &= \frac{\rho}{\tau} \lambda'^{ab} (\partial_\rho \omega'_b - 3\psi'_b \partial_\rho \mu' - \psi'_b \epsilon^{cd} \psi'_c \partial_\rho \psi'_d). \end{aligned} \quad (24)$$

We can show from Eq. (22) that Eq. (24) can be written as

$$\partial_\rho (a^1_\phi - a^1_\phi) = 0, \quad \partial_z (a^1_\phi - a^1_\phi) = 0. \quad (25)$$

Hence, a^1_ϕ can be obtained up to a constant as

$$\begin{aligned} \partial_\rho (A'_\phi - \sqrt{3} a^a_\phi \psi'_a) &= \sqrt{3} (-\psi'_a \partial_\rho a^a_\phi - \rho \tau'^{-1} (\partial_z \mu' + \epsilon^{ab} \psi'_a \partial_z \psi'_b)) \\ &= \sqrt{3} \rho \tau'^{-1} [\lambda'^{ab} \psi'_a \partial_z \omega'_b - (1 + 3\lambda'^{ab} \psi'_a \psi'_b) \partial_z \mu' - (1 + \lambda'^{ab} \psi'_a \psi'_b) \epsilon^{cd} \psi'_c \partial_z \psi'_d], \end{aligned} \quad (30)$$

where we have used Eq. (24) to eliminate $\partial_\rho a^a_\phi$ in the second line. The similar expression is obtained for the second equation in Eq. (29). Moreover, substituting Eq. (22) into the right-hand sides, this is expressed only in terms of the quantities of the vacuum seed solution

$$\begin{aligned} \partial_\rho (A'_\phi - \sqrt{3} a^a_\phi \psi'_a) &= \sqrt{3} [cs^2(\omega_0 \partial_\rho a^1_\phi - \rho \tau^{-1} \epsilon^{ab} \lambda_{0a} \partial_z \lambda_{b0}) - c^2 s \partial_\rho a^0_\phi], \\ \partial_z (A'_\phi - \sqrt{3} a^a_\phi \psi'_a) &= \sqrt{3} [cs^2(\omega_0 \partial_z a^1_\phi + \rho \tau^{-1} \epsilon^{ab} \lambda_{0a} \partial_\rho \lambda_{b0}) - c^2 s \partial_z a^0_\phi], \end{aligned} \quad (31)$$

$$a'^1_\phi = a^1_\phi. \quad (26)$$

Furthermore, Eq. (24) for $a = 0$ can be written as

$$\begin{aligned} \partial_\rho (a'^0_\phi - c^3 a^0_\phi) &= s^3 (-\omega_0 \partial_\rho a^1_\phi + \rho \tau^{-1} \epsilon^{cd} \lambda_{0c} \partial_z \lambda_{0d}), \\ \partial_z (a'^0_\phi - c^3 a^0_\phi) &= s^3 (-\omega_0 \partial_z a^1_\phi - \rho \tau^{-1} \epsilon^{cd} \lambda_{0c} \partial_\rho \lambda_{0d}), \end{aligned} \quad (27)$$

where we have used Eq. (11) corresponding to the vacuum seed solution before the Harrison transformation:

$$\partial_\rho a^a_\phi = -\frac{\rho}{\tau} \lambda^{ab} \partial_z \omega_b, \quad \partial_z a^a_\phi = \frac{\rho}{\tau} \lambda^{ab} \partial_\rho \omega_b. \quad (28)$$

Similarly, the gauge potential A'_ϕ is determined by

$$\begin{aligned} \partial_\rho A'_\phi &= \sqrt{3} (a^a_\phi \partial_\rho \psi'_a - \rho \tau'^{-1} (\partial_z \mu' + \epsilon^{ab} \psi'_a \partial_z \psi'_b)), \\ \partial_z A'_\phi &= \sqrt{3} (a^a_\phi \partial_z \psi'_a + \rho \tau'^{-1} (\partial_\rho \mu' + \epsilon^{ab} \psi'_a \partial_\rho \psi'_b)). \end{aligned} \quad (29)$$

One can rewrite the first equation of (29) as follows:

where we used Eq. (28) to eliminate the derivatives of ω_a on the right-hand side. Comparing with the right-hand side in Eq. (27), one can write this in the total derivative form, which results in

$$A'_\phi = \sqrt{3} \left(a'^a{}_\phi \psi'_a - \frac{c}{s} a'^0{}_\phi + \frac{c^2}{s} a^0{}_\phi \right). \quad (32)$$

Hence, integrating Eq. (27) is the only nontrivial task to obtain the charged metric. As will be seen later, this can be easily integrated in the C-metric, as in Ref. [14].

Therefore, one can derive the new metric and gauge potential describing the charged solution from Eqs. (2) and (3). This transformation adds an electric charge to a vacuum solution while preserving asymptotic flatness and Killing isometries. However, as noted in Ref. [14], performing the Harrison transformation on a regular vacuum black ring, such as the Pomeransky-Sen'kov solution, unavoidably leads to a Dirac-Misner string singularity appearing on the disk inside the ring. Conversely, the transformation can produce the regular Cvetič-Youm charged black hole from the vacuum black hole, such as the Myers-Perry solution. In our previous work [50], we solved this problem by utilizing a vacuum rotating black ring with a Dirac-Misner string singularity as the seed for the Harrison transformation and subsequently eliminating it appropriately by controlling the post-transformation parameters. As a result, we have obtained a regular exact solution for a non-BPS charged rotating black ring with a dipole charge. In the subsequent section, we will detail the procedure for utilizing a vacuum seed that includes a Dirac-Misner string singularity to derive a capped black hole solution.

III. CONSTRUCTION OF VACUUM SEED FOR HARRISON TRANSFORMATION

Pomeransky's pioneering work [53] marked the beginning of utilizing the inverse scattering method (ISM) [51,52] for constructing diverse vacuum solutions of five-dimensional black holes. This approach has since been employed in numerous studies [12,18,20–24,56–79], by using the rod structure [54,55]. In this section, we employ the ISM to craft the five-dimensional vacuum seed solution utilized for the electric Harrison transformation detailed in the subsequent section. This solution describes a vacuum rotating black lens with a Dirac-Misner string singularity, comprising a rotating black ring and a rotating black hole, with a horizon cross section of $L(n; 1) = S^3/\mathbb{Z}_n$ topology.

A. ISM construction of the vacuum seed

As a vacuum seed for the Harrison transformation, we choose the vacuum rotating black lens with a horizon cross section of lens space $L(n; 1)$ ($n = 0, 1, 2, \dots$), which initially possesses a Dirac-Misner string singularity. This

singularity will be eliminated by appropriately adjusting the parameters of the solution after the Harrison transformation. To construct this vacuum solution, we follow the procedure outlined for the vacuum rotating black lens by Chen and Teo [22]. The key distinction lies in the treatment of the Dirac-Misner string singularity: while they remove it, we retain it in our solution.

To use the ISM, we rewrite the Weyl-Papapetrou form (4) as

$$ds^2 = G_{ij} dx^i dx^j + f(d\rho^2 + dz^2), \quad (33)$$

where $(x^i) = (t, \psi, \phi)$ ($i = 0, 1, 2$), and a 3×3 matrix G_{ij} and f are the functions of ρ and z , with the constraint $\det(G_{ij}) = -\rho^2$. We begin with the diagonal metric given by

$$G_0 = \text{diag} \left(-\frac{\mu_0}{\mu_2}, \frac{\mu_2 \mu_3}{\mu_1}, \frac{\rho^2 \mu_1}{\mu_0 \mu_3} \right),$$

$$f_0 = \frac{C_f \mu_2 \mu_3 R_{01} R_{02} R_{12} R_{13}^2}{\mu_1 R_{00} R_{03} R_{11} R_{22} R_{23} R_{33}}, \quad (34)$$

where $\mu_i := \sqrt{\rho^2 + (z - z_i)^2} - z + z_i$ and $R_{ij} := \rho^2 + \mu_i \mu_j$. The rod structure is displayed in Fig. 1, and the constant C_f is consistently set to 1 throughout this paper. The $\psi\psi$ component of the metric diverges as $g_{\psi\psi} \sim \mathcal{O}(\rho^{-2})$ as $\rho \rightarrow 0$ for $z_1 < z < z_2$. This divergence indicates naked curvature singularities on the negative rod $\rho = 0, z_1 < z < z_2$, as discussed in Ref. [55].

Then, following Pomeransky's procedure [22,53], we first remove three trivial solitons from the points $z = z_0, z_2, z_3$ with vectors $(0, 0, 1)$, $(1, 0, 0)$, and $(0, 0, 1)$, respectively. Next, we add back three nontrivial solitons at the same points $z = z_0, z_2, z_3$ with vectors $m_{0,0} = (C_0, 0, 1)$, $m_{2,0} = (1, C_2, 0)$, and $m_{3,0} = (0, C_3, 1)$, respectively. For the diagonal metric, removing a trivial soliton corresponds to multiplying $-\mu_k^2/\rho^2$ to the kk component of G_0 , where k is the index of the nonzero component in the vector.

$$\begin{aligned} \tilde{G}_0 &= \text{diag} \left(-\frac{\mu_2^2}{\rho^2}, 1, \frac{\mu_0^2 \mu_3^2}{\rho^2 \rho^2} \right) G_0 \\ &= \text{diag} \left(\frac{\mu_0 \mu_2}{\rho^2}, \frac{\mu_2 \mu_3}{\mu_1}, \frac{\mu_0 \mu_1 \mu_3}{\rho^2} \right) \\ &= \text{diag} \left(\frac{\rho^2}{\bar{\mu}_0 \bar{\mu}_2}, \frac{\rho^4}{\mu_1 \bar{\mu}_2 \bar{\mu}_3}, \frac{\rho^2 \mu_1}{\bar{\mu}_0 \bar{\mu}_3} \right), \end{aligned} \quad (35)$$

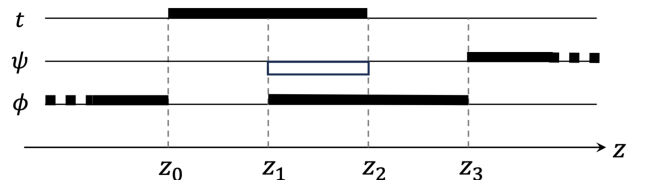


FIG. 1. Rod structure of the diagonal seed for the ISM.

where $\bar{\mu}_i := -\sqrt{\rho^2 + (z - z_i)^2} - z + z_i$ and we used $\mu_i \bar{\mu}_i = -\rho^2$ in the last line for the later use. The three-soliton solution is obtained from the modified metric \tilde{G}_0 and the vectors m_i as

$$G_3 = \tilde{G}_0 - \sum_{i,j=0,2,3} (\Gamma^{-1})_{ij} \frac{(m_i \tilde{G}_0) \otimes (m_j \tilde{G}_0)}{\mu_i \mu_j}, \quad (36)$$

$$\Psi_0(\lambda, \rho, z) = \text{diag} \left(\frac{\rho^2 - 2\lambda z - \lambda^2}{(\lambda - \bar{\mu}_0)(\lambda - \bar{\mu}_2)}, \frac{(\rho^2 - 2\lambda z - \lambda^2)^2}{(\mu_1 - \lambda)(\bar{\mu}_2 - \lambda)(\bar{\mu}_3 - \lambda)}, \frac{(\lambda - \mu_1)(\rho^2 - 2\lambda z - \lambda^2)}{(\lambda - \bar{\mu}_0)(\lambda - \bar{\mu}_3)} \right). \quad (38)$$

The metric function f can be obtained as

$$f_3 = \frac{\det(\Gamma_{ij})}{\det(\Gamma_{ij})|_{C_0, C_2, C_3 \rightarrow 0}} f_0. \quad (39)$$

To remove the divergence of the metric on $\rho = 0$, $z_1 < z < z_2$, we set

$$C_2 = \sqrt{\frac{2z_{20}}{z_{21}z_{32}}} z_2, \quad (40)$$

where $z_{ij} := z_i - z_j$. Under this condition (40), the rod vectors on two rods $\{(\rho, z) | \rho = 0, z_1 < z < z_2\}$ and $\{(\rho, z) | \rho = 0, z_2 < z < z_3\}$ become parallel, merging these rods into a single rod. Note that under this condition, the point $(\rho, z) = (0, z_2)$ no longer becomes an endpoint of the rods but a mere regular point, often referred to as a phantom point.

For later convenience, we introduce the following parameters:

$$b := C_0 \frac{z_{10}}{z_{30}} \sqrt{\frac{2z_{20}z_{32}}{z_{21}}}, \quad a := C_3 \frac{z_{31}^2}{z_{33}z_{30}} - C_0 \frac{z_{10}}{z_{30}} \sqrt{\frac{2z_{20}z_{21}}{z_{32}}}. \quad (41)$$

The resulting solution becomes asymptotically flat at $\sqrt{\rho^2 + z^2} \rightarrow \infty$ if and only if

$$-1 < a < 1, \quad (42)$$

or otherwise the spacetime is not Lorentzian, since the spatial metric $(G_3)_{IJ}$ ($I, J = \psi, \phi$) approaches a semipositive definite metric multiplied by the factor $(1 - a^2)^{-1}$ at infinity. Together with this condition, the solution turns out to asymptote to the standard Minkowski metric

where the 3×3 matrix Γ_{ij} is given by

$$\Gamma_{ij} := \frac{m_i \tilde{G}_0 m_j}{R_{ij}}, \quad m_i := m_{i,0} \Psi_0^{-1}(\lambda = \mu_i, \rho, z), \quad (i, j = 0, 2, 3), \quad (37)$$

with the generating matrix made from \tilde{G}_0 by the replacement $\mu_i \rightarrow \mu_i - \lambda$, $\bar{\mu}_i \rightarrow \bar{\mu}_i - \lambda$, $\rho^2 \rightarrow \rho^2 - 2\lambda z - \lambda^2$

under the global rotation, which is expressed as the coordinate change:

$$x^i \rightarrow \Lambda^i_j x^j, \quad (43)$$

where

$$\Lambda = \begin{pmatrix} 1 & -\Gamma_1 \Gamma_2 & b \Gamma_1 \Gamma_2 \\ 0 & \Gamma_1 & -a \Gamma_1 \\ 0 & -a \Gamma_1 & \Gamma_1 \end{pmatrix}, \quad \Gamma_1 := \frac{1}{\sqrt{1 - a^2}}, \quad \Gamma_2 := \sqrt{\frac{2z_{20}z_{21}}{z_{32}}}. \quad (44)$$

B. Vacuum seed solution for Harrison transformation

Under the condition (40), the metric can be written in the simpler form without square root terms if we introduce the C-metric coordinates (x, y) [55], which are defined as

$$\rho = \frac{2\ell^2 \sqrt{-G(x)G(y)}}{(x-y)^2}, \quad z = \frac{\ell^2(1-xy)(2+\nu(x+y))}{(x-y)^2}, \quad (45)$$

with the cubic function

$$G(u) = (1-u^2)(1+\nu u). \quad (46)$$

The endpoints z_i ($i = 0, 1, 2, 3$) of the rods are replaced by the new parameters ℓ, ν, γ

$$z_0 = -\nu \ell^2, \quad z_1 = \nu \ell^2, \quad z_2 = \gamma \ell^2, \quad z_3 = \ell^2, \quad (47)$$

where

$$\ell > 0, \quad \nu < \gamma < 1. \quad (48)$$

From the definition of the C-metric coordinates (x, y) , it appears that there is an invariance under the exchange

$(x, y) \rightarrow (y, x)$. However, the functions μ_i ($i = 0, 1, 3$)—which contribute to the metric—do not exhibit such symmetry due to the differences in their ranges, as indicated in Eq. (58) below. Consequently the functions including nasty square roots are written as rational functions of x and y ,

$$\mu_0 = -\frac{2\ell^2(1-x)(1+y)(1+\nu y)}{(x-y)^2}, \quad \mu_1 = -\frac{2\ell^2(1-x)(1+\nu x)(1+y)}{(x-y)^2}, \quad \mu_3 = \frac{2\ell^2(1+\nu x)(y^2-1)}{(x-y)^2}. \quad (49)$$

By the use of Eq. (40), the square root $\sqrt{\rho^2 + (z-z_2)^2}$ in μ_2 can be removed from the metric, and hence the point $z = z_2$ is referred to as a phantom point.

Finally, the metric of the vacuum solution in the C-metric form can be written as

$$ds^2 = -\frac{H(y, x)}{H(x, y)} (dt + \Omega_\psi(x, y)d\psi + \Omega_\phi(x, y)d\phi)^2 + \frac{F(y, x)}{H(y, x)} d\psi^2 - \frac{2J(x, y)}{H(y, x)} d\psi d\phi - \frac{F(x, y)}{H(y, x)} d\phi^2 + \frac{\ell^2 H(x, y)}{4(1-\gamma)^3(1-\nu)^2(1-a^2)(x-y)^2} \left(\frac{dx^2}{G(x)} - \frac{dy^2}{G(y)} \right), \quad (50)$$

where

$$H(x, y) = 2d_1(1-\gamma)(1-\nu)(2+\nu(1+x+y-xy))(\gamma(1+y)(1+\nu x) - 2 - \nu(3x+\nu+y(2+x+\nu+2x\nu))) + d_1c_3(1+\nu)(\gamma+\gamma\nu x - \nu(x+\nu))(1+x)(1+y)^2 + (1-\gamma)(1-\nu)^2(x+y+\nu+\nu xy)[2((1-\gamma)(1-\nu)(\gamma+\nu) - 2d_2)(2+\nu(1+x+y-xy)) + [2(\gamma-\nu)(2+(x+y)\nu) + (1-xy)((3-\nu)\nu+\gamma(1+\nu)) - (1-\nu)(\gamma+\nu)(x-y)]c_3], \quad (51)$$

$$F(x, y) = \frac{2\ell^2}{(1-a^2)(x-y)^2} \left[4[(1-a^2)^2(y-1)(1-\gamma)^3(1-\nu)^3 - d_1^2(1+y)](1+\nu y)G(x) + 4[(1-\nu)c_2 - (1-ab)(\gamma-\nu)(1+\nu)c_1]^2(1+\nu x)(1+x)G(y) + \nu^{-1}(1-\nu)^3(\gamma-\nu)(d_3^2(1-x^2)G(y) - c_3^2(1-y^2)G(x)) + \frac{G(x)G(y)[(1-a^2)(1-\gamma)d_4 - (a-b)^2y(1-\gamma)^2(\gamma-\nu)\nu c_2^2 + x(\gamma-\nu)\nu(bd_1 - c_1c_3)^2]}{\nu(1-\gamma)} \right], \quad (52)$$

$$J(x, y) = \frac{2\ell^2(1+x)(1+y)}{(1-a^2)(x-y)} [4d_1((a-b)(1-\gamma)(\gamma-\nu)(1+\nu) - ad_2)(1+\nu x)(1+\nu y) - d_3c_3(1-\nu)^3(\gamma-\nu)(1-x)(1-y) - (a-b)(\gamma-\nu)c_2(c_1c_3 - bd_1)(1-x)(1-y)(1+\nu x)(1+\nu y)], \quad (53)$$

$$\Omega_\psi(x, y) = \frac{v_0\ell(1+y)(1-\nu)}{\nu H(y, x)} [c_2(c_1c_3 - bd_1)(1-x)(1+\nu x)(1+\nu y) - (1-\nu)^2d_2c_3(1-x) + (1+x\nu)d_1(2\nu(1-ab)(1-\gamma)(1+\nu)(1+x) + (1-3\nu-x(1+\nu))c_3)], \quad (54)$$

$$\Omega_\phi(x, y) = \frac{v_0\ell(1+x)}{H(y, x)} \left[b(1+x)d_1(d_2(1+y)(1+\nu y) + \nu c_3(1-y^2)(1-\nu)) + \frac{2(a-b)(1-\gamma)^2(2d_1(1+\nu x)(1+\nu y)^2 - (1-\nu)^2\nu c_3(1-y)(x+y+\nu+\nu xy))}{1+\nu} \right], \quad (55)$$

and the coefficients are given by

$$\begin{aligned}
v_0 &:= \sqrt{\frac{2(\gamma^2 - \nu^2)}{(1 - a^2)(1 - \gamma)}}, \\
c_1 &:= (1 - \gamma)a + (\gamma - \nu)b, \\
c_2 &:= 2a(1 - \gamma)\nu + b(\gamma - \nu)(1 + \nu), \\
c_3 &:= 2(1 - \gamma)\nu + b^2(\gamma - \nu)(1 + \nu), \\
d_1 &:= (\nu + 1)c_1^2 - (1 - \gamma)(1 - \nu)^2, \\
d_2 &:= b(\nu + 1)c_1(\gamma - \nu) + 2\nu(1 - \gamma)(1 - \nu), \\
d_3 &:= (a^2 - 1)b(\gamma - 1)(\nu + 1) - ac_3, \\
d_4 &:= b^2(\gamma - \nu)[(\nu + 1)^2c_1^2(-3(1 - \gamma)\nu - \nu^2 + 1) - (1 - \gamma)(1 - \nu)^4(2\nu + 1)] \\
&\quad + (1 - \gamma)[((1 - \nu)c_2 - 2\nu^2c_1)^2 - 4\nu^2c_1^2(-\gamma(\nu + 2) + 3\nu^2 + 1)].
\end{aligned} \tag{56}$$

We assume the ranges of the coordinates as

$$-\infty < t < \infty, \quad 0 \leq \psi \leq 2\pi, \quad 0 \leq \phi \leq 2\pi, \tag{57}$$

and

$$-1 \leq x \leq 1, \quad -1/\nu \leq y \leq -1, \tag{58}$$

where the boundary of the coordinate (x, y) corresponds to the rods plus infinity:

- (i) ϕ -rotational axis: $\partial\Sigma_\phi = \{(x, y) | x = -1, -1 < y < -1/\nu\}$ with the rod vector $v_\phi := (0, 0, 1)$, where in the choice of $C_f = 1$, the periodicity $\phi \sim \phi + 2\pi$ from the coordinate ranges (57) ensures the absence of the conical singularities,
- (ii) Horizon: $\partial\Sigma_{\mathcal{H}} = \{(x, y) | -1 < x < 1, y = -1/\nu\}$ with the rod vector $v_{\mathcal{H}} := (1, \omega_\psi^{\text{vac}}, \omega_\phi^{\text{vac}})$, where

$$\begin{aligned}
\omega_\psi^{\text{vac}} &= \frac{v_0(1 - a^2)(1 - \gamma)}{2\ell(\gamma + \nu)(1 - a^2 + a(a - b)\gamma - (1 - ab)\nu)}, \\
\omega_\phi^{\text{vac}} &= \omega_\psi^{\text{vac}} \frac{2a(1 - \gamma)\nu - (1 - a^2)b(1 - \gamma)(1 + \nu) + ab^2(\gamma - \nu)(1 + \nu)}{2(1 - \gamma)\nu + b^2(\gamma - \nu)(1 + \nu)},
\end{aligned} \tag{59}$$

- (iii) Inner axis: $\partial\Sigma_{\text{in}} = \{(x, y) | x = 1, -1 < y < -1/\nu\}$ with the rod vector

$$v_{\text{in}} := (v_0\ell(a - b), n, 1), \tag{60}$$

with

$$n := \frac{ad_1 + (1 - \gamma)(1 + \nu)(1 - a^2)c_1}{d_1}, \tag{61}$$

where we note that the presence of the t component denotes the existence of the Dirac-Misner string singularity [80],

- (iv) ψ -rotational axis: $\partial\Sigma_\psi = \{(x, y) | -1 < x < 1, y = -1\}$ with the rod vector $v_\psi := (0, 1, 0)$, where the periodicity $\psi \sim \psi + 2\pi$ from the coordinate ranges (57) also ensures the absence of the conical singularities,
- (v) Infinity: $\partial\Sigma_\infty = \{(\rho, z) | \sqrt{\rho^2 + z^2} \rightarrow \infty \text{ with } z/\sqrt{\rho^2 + z^2} \text{ finite}\} = \{(x, y) | x \rightarrow y \rightarrow -1\}$.

As studied earlier in Ref. [22], setting $a = b$ and imposing regularity conditions, in which the obtained metric exactly describes the rotating black lens in [22], allows us to remove the Dirac-Misner string singularity [80] on the inner axis $\partial\Sigma_{\text{in}}$. However, similar to the approach taken for the charged dipole black ring in Ref. [50], we choose to use the vacuum black lens possessing a Dirac-Misner string singularity as the seed for the Harrison transformation. Hence, we do not assume its absence ($a \neq b$) before the Harrison transformation. In the following section, we will eliminate it after the transformation by appropriately adjusting the solution's parameters.

IV. CHARGED SOLUTION FROM HARRISON TRANSFORMATION

Now, let us utilize the electric Harrison transformation (22) on the vacuum solution (50) derived in the previous section. The procedure to obtain the charged solution follows a similar approach to that used for the charged black ring [14,50]. First, we express the vacuum

solution (50) in terms of eight scalar potentials $\Phi^A = (\lambda_{ab}, \omega_a, \psi_a, \mu)$. Since the vacuum solution possesses two axial Killing vectors $\partial/\partial\psi$ and $\partial/\partial\phi$, there are two possible ways to express the solution in terms of the potentials, depending on the following choice of the Killing vectors: (i) $\xi_0 = \partial/\partial t$, $\xi_1 = \partial/\partial\psi$, $\xi_2 = \partial/\partial\phi$ and (ii) $\xi_0 = \partial/\partial t$, $\xi_1 = \partial/\partial\phi$, $\xi_2 = \partial/\partial\psi$.

In case (i), from the metric (50), we can extract λ_{ab} , a^a_ϕ and τ , expressed as

$$\begin{aligned} \lambda_{00} &= -\frac{H(y, x)}{H(x, y)}, & \lambda_{01} &= -\frac{H(y, x)}{H(x, y)}\Omega_\psi(x, y), & \lambda_{11} &= \frac{F(y, x)}{H(y, x)} - \frac{H(y, x)}{H(x, y)}\Omega_\psi^2(x, y). \\ a^0_\phi &= \Omega_\phi(x, y) + \frac{J(x, y)}{F(y, x)}\Omega_\psi(x, y), & a^1_\phi &= -\frac{J(x, y)}{F(y, x)}, & \tau &= \frac{F(y, x)}{H(x, y)}. \end{aligned} \quad (62)$$

The twist potential ω_a can be obtained by directly integrating Eq. (28). This yields

$$\omega_0 = -\Omega_\phi(y, x), \quad (63)$$

$$\omega_1 = -\frac{J(x, y) + K(x, y)}{H(x, y)}, \quad (64)$$

where $K(x, y)$ is a polynomial of x and y :

$$\begin{aligned} K(x, y) &= \frac{\ell^2(1+y)}{1-a^2} [k_1(1-x^2)(1+y) + k_2\{(1+x)(1-y)(1+\nu x) + (1-x)(1+y)(1+\nu y)\} \\ &\quad + k_3(x-y)(\nu xy - x - y - 1) - 2) + k_4(1-x)(1-y)(\nu(x-y-1) + 1) \\ &\quad + k_5(1-x)(1-y) + k_6\{(\nu+1)^2(x+1)(y+1) - 4(1+\nu x)(1+\nu y)\} + k_7(1+\nu x)(1+\nu y)], \end{aligned} \quad (65)$$

in which the coefficients k_i ($i = 1, \dots, 7$) are given in Appendix A. In case (ii), we denote the corresponding quantities with ‘‘hats,’’ which can be expressed as

$$\begin{aligned} \hat{\lambda}_{00} &= -\frac{H(y, x)}{H(x, y)}, & \hat{\lambda}_{01} &= \frac{H(y, x)}{H(x, y)}\Omega_\phi(x, y), & \hat{\lambda}_{11} &= -\frac{F(x, y)}{H(y, x)} - \frac{H(y, x)}{H(x, y)}\Omega_\phi^2(x, y), \\ \hat{a}^0_\psi &= \Omega_\psi(x, y) - \frac{J(x, y)}{F(x, y)}\Omega_\phi(x, y), & \hat{a}^1_\psi &= \frac{J(x, y)}{F(x, y)}, & \hat{\tau} &= -\frac{F(x, y)}{H(x, y)}, \end{aligned} \quad (66)$$

which yields

$$\hat{\omega}_0 = \Omega_\psi(y, x), \quad (67)$$

$$\hat{\omega}_1 = \frac{J(x, y) + \hat{K}(x, y)}{H(x, y)}, \quad (68)$$

where $\hat{K}(x, y)$ can be expressed, in terms of $K(x, y)$, as

$$\hat{K}(x, y) = -K(y, x) - \frac{2\ell^2 c_3 d_1 (1-\nu)(x+1)^2(\gamma+\nu)(2a(1-\gamma)(1-\nu) + c_2(y+1))}{(1-a^2)(1-\gamma)}. \quad (69)$$

When deriving the metric and gauge potential after the Harrison transformation, the most nontrivial aspect lies in determining a^0_ϕ or \hat{a}^0_ψ through the integration of Eq. (27), resulting in

$$a^0_\phi = c^3 a^0_\phi(x, y) - s^3 \hat{a}^0_\psi(y, x), \quad (70)$$

$$\hat{a}^0_\psi = c^3 \hat{a}^0_\psi(x, y) + s^3 a^0_\phi(y, x), \quad (71)$$

which also has the same form as that of the vacuum doubly rotating black ring. The metric functions a^0_ϕ and \hat{a}^0_ψ in cases (i) and (ii) are intertwined in the transformed metric. This highlights that the two Harrison transformations of (i)

and (ii) are connected through sign flips: $s \rightarrow -s$, $t \rightarrow -t$, $\psi \rightarrow -\psi$, and $\phi \rightarrow -\phi$. Therefore, in what follows, we consider only the Harrison transformation in case (i).

Since Eq. (10) is invariant under the transformation, the function σ is also invariant. Then, from the change of τ in Eq. (22), one can see that the two-dimensional conformal factor in Eq. (4) is multiplied by D , which leads to

$$ds^2 = -\frac{H(y,x)}{D^2 H(x,y)}(dt + \Omega')^2 + D \left[\frac{F(y,x)}{H(y,x)} d\psi^2 - \frac{2J(x,y)}{H(y,x)} d\psi d\phi - \frac{F(x,y)}{H(y,x)} d\phi^2 \right] + \frac{\ell^2 D H(x,y)}{4(1-\gamma)^3(1-\nu)^2(1-a^2)(x-y)^2} \left(\frac{dx^2}{G(x)} - \frac{dy^2}{G(y)} \right), \quad (73)$$

$$A = \frac{\sqrt{3}cs}{DH(x,y)} [(H(x,y) - H(y,x))dt - (cH(y,x)\Omega_\psi(x,y) - sH(x,y)\Omega_\phi(y,x))d\psi - (cH(y,x)\Omega_\phi(x,y) - sH(x,y)\Omega_\psi(y,x))d\phi], \quad (74)$$

where the functions D , Ω'_ψ , and Ω'_ϕ are given by

$$D = \frac{c^2 H(x,y) - s^2 H(y,x)}{H(x,y)}, \quad (75)$$

$$\Omega' = (c^3 \Omega_\psi(x,y) - s^3 \Omega_\phi(y,x))d\psi + (c^3 \Omega_\phi(x,y) - s^3 \Omega_\psi(y,x))d\phi. \quad (76)$$

The Harrison transformation (22) changes the rod structure of the vacuum solution as follows (see Fig. 2 about the rod diagram):

- (i) ϕ -rotational axis: $\partial\Sigma_\phi = \{(x,y)|x = -1, -1/\nu < y < -1\}$ with the rod vector $v_\phi = (0, 0, 1)$. The periodicity of $\phi \sim \phi + 2\pi$ still leaves the absence of conical singularities.

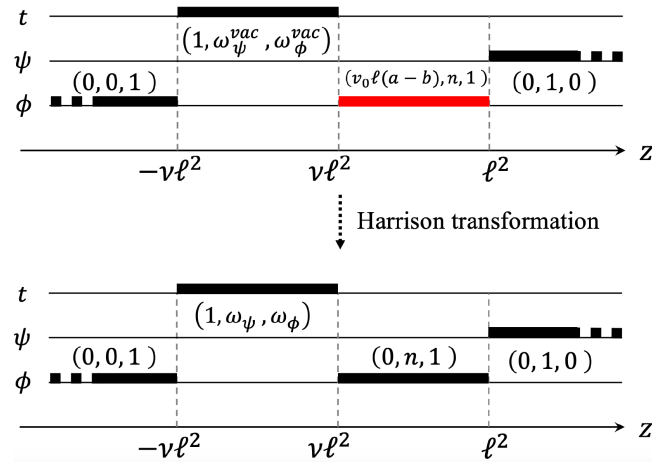


FIG. 2. The rod structures before and after applying the Harrison transformation, with the condition (79) imposed on the latter.

$$g'_{xx} = Dg_{xx}, \quad g'_{yy} = Dg_{yy}. \quad (72)$$

A. Charged solution

In case (i), the metric and gauge potential for a charged solution in five-dimensional minimal supergravity after the electric Harrison transformation can be written as

- (ii) Horizon: $\partial\Sigma_{\mathcal{H}} = \{(x,y)|-1 < x < 1, y = -1/\nu\}$ with the rod vector $v_{\mathcal{H}} = (1, \omega_\psi, \omega_\phi)$, with

$$\omega_\psi = \frac{v_0(1-a^2)(1-\gamma)}{2\ell(\gamma+\nu)[c^3(1-\nu-ac_1) - s^3(a-b)(\gamma-\nu)]},$$

$$\omega_\phi = -\frac{d_3\omega_\psi}{c_3}. \quad (77)$$

- (iii) Inner axis: $\partial\Sigma_{\text{in}} = \{(x,y)|x = 1, -1/\nu < y < -1\}$ with the rod vector

$$v_{\text{in}} = (v_0\ell(c^3(a-b) - s^3(1-ab)), n, 1), \quad (78)$$

where n is given by Eq. (61).

- (iv) ψ -rotational axis: $\partial\Sigma_\psi = \{(x,y)|-1 < x < 1, y = -1\}$ with the rod vector $v_\psi = (0, 1, 0)$. The periodicity of $\psi \sim \psi + 2\pi$ still leaves the absence of conical singularities,

- (v) Infinity: $\partial\Sigma_\infty = \{(x,y)|x \rightarrow y \rightarrow -1\}$.

One can see that the Harrison transformation preserves both the positions and the regularity of the ϕ - and ψ -rotational axes at $x = -1$ and $y = -1$, respectively. The event horizon remains at $y = -1/\nu$ but the horizon velocities are changed. The rod vector of the inner axis $\partial\Sigma_{\text{in}}$ changes from $(v_0\ell(a-b), n, 1)$ to $(v_0\ell(c^3(a-b) - s^3(1-ab)), n, 1)$, which enables one to eliminate the Dirac-Misner string singularity by setting

$$\tanh^3 \alpha = \frac{a-b}{1-ab}, \quad (79)$$

where the vacuum case corresponds to $a = b$. As seen in Ref. [50], the Dirac-Misner string singularity is unavoidable if we transform the vacuum seed not possessing the

Dirac-Misner string singularity (the vacuum seed corresponding to $a = b$). From the range (42) of a and $-1 < \alpha < 1$, the parameter b runs the range

$$-1 < b < 1. \quad (80)$$

Under the condition (79) for the absence of the Dirac-Misner string singularity, the rod vector on $\partial\Sigma_{\text{in}}$ becomes $\partial_{\phi'} = \partial_{\phi} + n\partial_{\psi}$, and the absence of conical singularities requires

$$\left(\frac{\Delta\phi'}{2\pi}\right)^2 = \frac{d_1^2}{(1-a^2)^2(1-\gamma)^3(1-\nu)^2(1+\nu)} = 1. \quad (81)$$

The topology condition for $\partial\Sigma_{\mathcal{H}}$ requires

$$\det(\hat{v}_{\text{in}}, \hat{v}_{\psi}) = \frac{ad_1 + (1-\gamma)(1+\nu)(1-a^2)c_1}{d_1} = n \in \mathbb{Z}, \quad (82)$$

where each hatted vector \hat{v} denotes a two-dimensional vector made from ψ and ϕ components of each rod vector v . As proved in Ref. [17], the horizon cross section has the topology of $S^2 \times S^1$ for $n = 0$, S^3 for $n = \pm 1$ and $L(n; 1)$ for $|n| \geq 2$. To study all possibilities, we do not fix the value of n here.

To summarize, the charged solution has six parameters $(\ell, a, b, \gamma, \nu, \alpha)$, with the following ranges:

$$\begin{aligned} \ell > 0, \quad -1 < a < 1, \quad -1 < b < 1, \\ 0 < \nu < \gamma < 1, \quad -\infty < \alpha < \infty. \end{aligned} \quad (83)$$

The regularity of the metric at each boundary imposes the conditions (79), (81), and (82), which reduce the independent parameters of the solution from six to three. Moreover, the solution and the conditions are invariant under transformations $n \rightarrow -n$, $a \rightarrow -a$, $b \rightarrow -b$, $\alpha \rightarrow -\alpha$, and hence we may assume $n \geq 0$ without loss of generality. In the following, under the conditions (79), (81), and (82), we investigate whether the charged solution has curvature singularities and CTCs for each value of n .

B. Regularity at the coordinate boundaries

Curvature singularities on and outside the horizon may arise at points where the metric and its inverse appear to diverge in the range (58). This occurs on the surfaces $H(x, y) = 0$ and $D = 0$, as well as on the boundary of the C-metric coordinates at $x = \pm 1$ and $y = -1/\nu, -1$, where $G(x) = 0$ or $G(y) = 0$. From $H(-1, -1) = 8(1-\gamma)^3(1-\nu)^4(1-a^2) > 0$ and $D = 1$ at infinity $x \rightarrow y \rightarrow -1$. Hence, the necessary and sufficient condition for the absence of surfaces $H(x, y) = 0$ and $D = 0$ is that $H(x, y)$ and D are positive everywhere in the range (58). Since the discussion regarding $H(x, y) > 0$ and $D > 0$ depends on the value of n , we will address this in the next subsection. Here, we

demonstrate the absence of curvature singularities at the coordinate boundaries, $x = \pm 1$, $y = -1, -1/\nu$, by assuming $H(x, y) > 0$ and $D > 0$. Additionally, we notice that despite its appearance in the metric (73), the surface $H(y, x) = 0$ does not cause a divergence in the metric and its inverse. This is because the factor $H^{-1}(y, x)$ does not appear in each component of $g_{\mu\nu}$ and $g^{\mu\nu}$.

- (1) The limit $x \rightarrow y \rightarrow -1$ corresponds to the asymptotic infinity. In terms of the standard spherical coordinates (r, θ) defined as

$$\begin{aligned} x &= -1 + 4(1-\nu)\ell^2 r^{-2} \cos^2 \theta, \\ y &= -1 - 4(1-\nu)\ell^2 r^{-2} \sin^2 \theta, \end{aligned} \quad (84)$$

we find that the metric at $r \rightarrow \infty$ ($x \rightarrow y \rightarrow -1$) behaves as the Minkowski metric:

$$ds^2 \simeq -dt^2 + dr^2 + r^2(d\theta^2 + \sin^2 \theta d\psi^2 + \cos^2 \theta d\phi^2). \quad (85)$$

Hence, the charged metric (73) describes an asymptotically flat spacetime.

- (2) The point $(x, y) = (1, -1)$ corresponds to a center of the spacetime, i.e., the intersection of the ψ -rotational axis and inner rotational axis. Using the coordinates (r, θ) introduced by

$$\begin{aligned} x &= 1 - \frac{(1+\nu)(1-\gamma)^2(1-a^2)r^2 \cos^2 \theta}{|d_1|\ell^2(1+c^2\nu+s^2\gamma)}, \\ y &= -1 - \frac{(1-\nu)(1-\gamma)^2(1-a^2)r^2 \sin^2 \theta}{|d_1|\ell^2(1+c^2\nu+s^2\gamma)}, \end{aligned} \quad (86)$$

we can show that the metric at $r \rightarrow 0$ [$(x, y) \rightarrow (1, -1)$] behaves as the origin of the Minkowski spacetime written in the spherical coordinates if $d_1 < 0$,

$$ds^2 \simeq -dt'^2 + (-d_1/|d_1|)[dr^2 + r^2(d\theta^2 + \sin^2 \theta d\psi'^2 + \cos^2 \theta d\phi^2)], \quad (87)$$

where $t' := \sqrt{(1-\gamma)(1+\nu)}t/(1+c^2\nu+s^2\gamma)$ and $\psi' = \psi - n\phi$.

If $d_1 > 0$, the metric is not Lorentzian around this point but the negativity of d_1 is ensured by the positivity of $H(x, y)$ at this point, since

$$H(1, -1) = -8d_1(1-\gamma)(1-\nu)(1-\nu^2) > 0 \Leftrightarrow d_1 < 0. \quad (88)$$

Under this condition, the point $(x, y) = (1, -1)$ is regular.

- (3) The boundaries $x = -1$ and $x = 1$ correspond to the ϕ -rotational axis and inner rotational axes, respectively. Introducing the radial coordinate r by $x = \pm 1 \mp C_{\pm} r^2$ with positive constants C_{\pm} for $x = \pm 1$, we can see that, with the use of Eqs. (82) and (81), the metric at $r \rightarrow 0$ ($x \rightarrow \pm 1$) behaves as

$$ds^2 \simeq \gamma_{tt}^{\pm}(y) dt^2 + 2\gamma_{t\psi}^{\pm}(y) dt d\psi_{\pm} + \gamma_{\psi\psi}^{\pm}(y) d\psi_{\pm}^2 + \alpha_{\pm}(y) (dr^2 + r^2 d\phi_{\pm}^2 - G^{-1}(y) dy^2), \quad (89)$$

where

$$\begin{aligned} \gamma_{tt}^{\pm} &= -\frac{D|_{x=\pm 1} H(y, \pm 1)}{H(\pm 1, y)}, & \gamma_{\psi\psi}^{\pm} &= -\frac{H(y, \pm 1) [c^3 \Omega_{\phi}(\pm 1, y) - s^3 \Omega_{\psi}(y, \pm 1)]}{D^2|_{x=\pm 1} H(\pm 1, y)}, \\ \gamma_{\psi\psi}^{\pm} &= \frac{D|_{x=\pm 1} F(y, \pm 1)}{H(y, \pm 1)} - \frac{H(y, \pm 1) [c^3 \Omega_{\psi}(\pm 1, y) - s^3 \Omega_{\phi}(y, \pm 1)]^2}{D^2|_{x=\pm 1} H(\pm 1, y)}, \\ \alpha_{\pm} &= \frac{C_{\pm} \ell^2 D|_{x=\pm 1} H(\pm 1, y)}{2(1-\gamma)^3 (1 \pm \nu) (1-\nu)^2 (1-a^2) (1 \mp y)^2}, \end{aligned} \quad (90)$$

and

$$(\psi_-, \phi_-) := (\psi, \phi), \quad (\psi_+, \phi_+) := (\psi - n\phi, \phi). \quad (91)$$

Under the assumptions $H(x, y) > 0$ and $D > 0$, we can also show that $\alpha_{\pm} > 0$, and

$$\det(\gamma^+) = \frac{16\ell^2 d_1^2 (1+\nu)(1+y)(1+\nu y)}{(1-a^2)(1-y)D|_{x=1} H(1, y)} < 0, \quad (92)$$

$$\det(\gamma^-) = \frac{16\ell^2 (1-\gamma)^3 (1-\nu)^4 (1-a^2)(1-y)(1+\nu y)}{(1+y)D|_{x=-1} H(-1, y)} < 0, \quad (93)$$

hence γ^{\pm} is a nonsingular and nondegenerate matrix for $-1/\nu < y < -1$. Thus, the metric is regular at $x = \pm 1$.

- (4) The boundary $y = -1$ corresponds to the ψ -rotational axis. Introducing the radial coordinate r by $y = -1 - C_0 r^2$ with a positive constant C_0 , we can see that the metric at $r \rightarrow 0$ ($y \rightarrow -1$) behaves as

$$ds^2 \simeq \gamma_{tt}^0(x) dt^2 + 2\gamma_{t\phi}^0(x) dt d\phi + \gamma_{\phi\phi}^0(x) d\phi^2 + \alpha_0(x) (dr^2 + r^2 d\psi^2 + G^{-1}(x) dx^2), \quad (94)$$

where

$$\begin{aligned} \gamma_{tt}^0 &= -\frac{D|_{y=-1} H(-1, x)}{H(x, -1)}, & \gamma_{t\phi}^0 &= -\frac{H(-1, x) [c^3 \Omega_{\phi}(x, -1) - s^3 \Omega_{\psi}(-1, x)]}{D^2|_{y=-1} H(x, -1)}, \\ \gamma_{\phi\phi}^0 &= -\frac{D|_{y=-1} F(x, -1)}{H(-1, x)} - \frac{H(-1, x) [c^3 \Omega_{\phi}(x, -1) - s^3 \Omega_{\psi}(-1, x)]^2}{D^2|_{y=-1} H(x, -1)}, & \alpha_0 &= \frac{C_0 \ell^2 D|_{y=-1} H(x, -1)}{2(1-\gamma)^3 (1-\nu)^3 (1-a^2) (1+x)^2}. \end{aligned} \quad (95)$$

Under the assumptions of $H(x, y) > 0$ and $D > 0$, we can also show that $\alpha_0 > 0$ and

$$\det(\gamma^0) = -\frac{16\ell^2 (1-\gamma)^3 (1-\nu)^4 (1-a^2)(1-x)(1+\nu x)}{(1+x)D|_{y=-1} H(x, -1)} < 0, \quad (96)$$

and hence γ^0 is a nonsingular and nondegenerate matrix for $-1 < x < 1$. Therefore, the metric is also regular at $y = -1$.

- (5) The boundary $y = -1/\nu$ corresponds to a Killing horizon with the surface gravity

$$\kappa = \frac{(1-a^2)^{3/2} (1-\gamma)^2 \sqrt{\nu(1+\nu)(\gamma+\nu)^{-1}}}{c_3 \ell (c^3 (1-\nu - ac_1) + s^3 (b-a)(\gamma-\nu))}, \quad (97)$$

and the null generator is denoted by $v_{\mathcal{H}} = \partial/\partial t + \omega_\psi \partial/\partial \psi + \omega_\phi \partial/\partial \phi$ with

$$(\omega_\psi, \omega_\phi) = \frac{\kappa}{(1-a^2)} \sqrt{\frac{\gamma-\nu}{2\nu(1-\gamma)^3(1+\nu)}} (c_3, -d_3). \quad (98)$$

We can show that both the metric and gauge potential are regular at $y = -1/\nu$, introducing the ingoing/outgoing Eddington-Finkelstein coordinates by

$$dx^i = dx'^i \pm v_{\mathcal{H}}^i \frac{(1-\nu^2)}{2\nu\kappa G(y)} dy, \quad (99)$$

where $(x^i) = (t, \psi, \phi)$ ($i = 0, 1, 2$) and the metric near $y = -1/\nu$ behaves as

$$ds^2 \simeq \alpha_H(x) \left(\frac{4\nu^2 \kappa^2 G(y)}{(1-\nu^2)^2} dt'^2 \pm \frac{4\nu\kappa}{1-\nu^2} dt' dy + \frac{dx^2}{G(x)} \right) + \gamma_{\psi\psi}^H(x) (d\psi' - \omega_\psi dt')^2 + 2\gamma_{\psi\phi}^H(x) (d\psi' - \omega_\psi dt')(d\phi' - \omega_\phi dt') + \gamma_{\phi\phi}^H(x) (d\phi' - \omega_\phi dt')^2, \quad (100)$$

with

$$\begin{aligned} \gamma_{\psi\psi}^H &= \frac{D|_{y=-1/\nu} F(-1/\nu, x)}{H(-1/\nu, x)} - \frac{H(-1/\nu, x) [c^3 \Omega_\psi(x, -1/\nu) - s^3 \Omega_\phi(-1/\nu, x)]^2}{D^2|_{y=-1/\nu} H(x, -1/\nu)}, \\ \gamma_{\psi\phi}^H &= -\frac{D|_{y=-1/\nu} J(x, -1/\nu)}{H(-1/\nu, x)} - \frac{H(-1/\nu, x) [c^3 \Omega_\psi(x, -1/\nu) - s^3 \Omega_\phi(-1/\nu, x)] [c^3 \Omega_\phi(x, -1/\nu) - s^3 \Omega_\psi(-1/\nu, x)]}{D^2|_{y=-1/\nu} H(x, -1/\nu)}, \\ \gamma_{\phi\phi}^H &= -\frac{D|_{y=-1/\nu} F(x, -1/\nu)}{H(-1/\nu, x)} - \frac{H(-1/\nu, x) [c^3 \Omega_\phi(x, -1/\nu) - s^3 \Omega_\psi(-1/\nu, x)]^2}{D^2|_{y=-1/\nu} H(x, -1/\nu)}, \\ \alpha_H &= \frac{\ell^2 \nu^2 D|_{y=-1/\nu} H(x, -1/\nu)}{4(1-\gamma)^3 (1-\nu)^2 (1-a^2) (1+\nu x)^2}, \end{aligned} \quad (101)$$

and hence, under the assumptions $H(x, y) > 0$ and $D > 0$, we can show $\alpha_H > 0$ and

$$\det(\gamma^H) = \frac{4\ell^4 c_3^2 (1-\nu)^4 (\nu+1) (1-x^2) (\gamma+\nu) [c^3 (ac_1 + \nu - 1) - s^3 (b-a) (\gamma-\nu)]^2}{(1-a^2)^2 (1-\gamma) D|_{y=-1/\nu} \nu (\nu x + 1) H(x, -1/\nu)} > 0 \quad (102)$$

and thus γ^H is a nonsingular and nondegenerate matrix for $-1 < x < 1$. Hence, the metric is smoothly continued to $-\infty < y < -1/\nu$ across the horizon $y = -1/\nu$. Moreover, in the Eddington-Finkelstein coordinate, the gauge potential also remains regular at the horizon $y = -1/\nu$ under the gauge transformation

$$A' = A \pm d \left(\frac{(1-\nu^2) \Phi_e}{2\nu\kappa} \int \frac{dy}{G(y)} \right), \quad (103)$$

where Φ_e is the electric potential defined by

$$\Phi_e := -(A_t + A_\psi \omega_\psi + A_\phi \omega_\phi)|_{y=-1} = -\frac{\sqrt{3}cs((\gamma-1)(\nu+1)s(b-a)(\gamma-\nu) + c(d_1-d_2))}{(\gamma-1)(\nu+1)s^3(b-a)(\gamma-\nu) + c^3(d_1-d_2)}. \quad (104)$$

- (6) The points $(x, y) = (\pm 1, -1/\nu)$ correspond to the intersecting points of the rotational axes and the horizon. By introducing the coordinates (r, θ) for $(x, y) = (\pm 1, -1/\nu)$ as

$$x = \pm 1 \mp c_\pm r^2 \sin^2 \theta, \quad y = -\frac{1}{\nu} \left(1 - \frac{(1 \mp \nu) c_\pm}{2} r^2 \cos^2 \theta \right), \quad c_\pm: \text{positive constants}, \quad (105)$$

and with the use of Eqs. (81) and (82), the metric at $r \rightarrow 0$ ($(x, y) \rightarrow (\pm 1, -1/\nu)$) behaves as

$$ds^2 \simeq dr^2 + r^2 d\theta^2 + r^2 \sin^2 \theta (d\phi_{\pm} - \omega_{\phi} dt)^2 - r^2 \kappa^2 \cos^2 \theta dt^2 + R_{\pm}^2 (d\psi_{\pm} - \omega_{\psi}^{\pm} dt)^2, \quad (106)$$

where $\omega_{\psi}^+ = \omega_{\psi} - n\omega_{\phi}$, $\omega_{\psi}^- = \omega_{\psi}$, and (ψ_{\pm}, ϕ_{\pm}) are defined in Eq. (91). $R_{\pm} := \sqrt{g_{\psi\psi}|_{(x,y)=(\pm 1, -1/\nu)}}$ are given by

$$R_+ = \frac{2\ell(-d_1)(\gamma - \nu)\sqrt{\nu(\gamma + \nu)}(c^3 d_2 + bs^3(d_2 - (\gamma - 1)(\nu - 1)(\gamma + \nu)))}{\sqrt{(a^2 - 1)(\gamma - 1)(c^2 d_2^2(\gamma - \nu) + 2\nu s^2(d_2 - (\gamma - 1)(\nu - 1)(\gamma + \nu))^2)}, \quad (107)$$

$$R_- = \frac{2\ell\sqrt{\nu(\gamma + \nu)}(c^3(d_2 - d_1) - s^3(\gamma - 1)(\nu + 1)(b - a)(\gamma - \nu))}{(1 - \gamma)\sqrt{(1 - a^2)(\nu + 1)((\nu + 1)s^2(\gamma - \nu) - 2c^2(\gamma - 1)\nu)}}. \quad (108)$$

We also set c_{\pm} as

$$c_+ = \frac{(1 - a^2)\kappa((1 - \gamma)(\nu + 1))^{3/2}R_+}{2(-d_1)\nu\ell^2},$$

$$c_- = \frac{\kappa(1 - \nu)R_-}{2\nu(\nu + 1)\ell^2}. \quad (109)$$

Note that the negativity (88) of d_1 ensures that the metric is Lorentzian at $(x, y) = (1, -1/\nu)$. In the Cartesian coordinates $(T, X, Y, Z, W) = (\kappa t, r \cos \theta, r \sin \theta \cos(\phi_{\pm} - \omega_{\phi} t), r \sin \theta \sin(\phi_{\pm} - \omega_{\phi} t), R_{\pm}(\psi_{\pm} - \omega_{\psi}^{\pm} t))$, the above asymptotic metric becomes

$$ds^2 \simeq -X^2 dT^2 + dX^2 + dY^2 + dZ^2 + dW^2, \quad (110)$$

where the Rindler horizon lies at $X = 0$. Therefore, the metric is regular at $(x, y) = (\pm 1, -1/\nu)$.

C. Parameter regions for regularity

Since in the previous subsection, we have shown that there are no curvature singularities at the boundaries $x = \pm 1, y = -1, y = -1/\nu$ of the C-metric coordinates under the assumptions of $H(x, y) > 0$ and $D > 0$ in the coordinate ranges (58), now we investigate whether they can indeed be positive in the ranges (58). If $H(x, y) > 0$ and $D > 0$ everywhere in the ranges (58), curvature singularities do not appear on and outside the horizon. This depends on the value of n , and hence we classify the analysis into the following three cases: (i) $n = 0$ (a black ring), (ii) $n = 1$ (a black hole), (iii) $n \geq 2$ (a black lens). For this purpose, instead of using $H(x, y)$, it is more convenient to use the condition (88), which can be expressed from Eqs. (81) and (82) as

$$d_1 = (1 - \gamma)(1 - \nu)^2(n - 1 - a)(n + 1 - a) < 0. \quad (111)$$

This provides a necessary condition for the absence of the surface $H(x, y) = 0$, and curvature singularities exist if this condition is violated.

1. $n = 0$ (a black ring with $S^2 \times S^1$ -horizon topology)

For $n = 0$, the horizon cross section has the topology of $S^2 \times S^1$. In this case, we can show from Eq. (111) that $d_1 = -(1 - \gamma)(1 - \nu)^2(1 - a^2) < 0$ is always satisfied in the ranges of γ, ν, a (83). Moreover, we can solve Eqs. (79), (81), and (82) as

$$b = 0, \quad \gamma = \frac{\nu(3 - \nu)}{1 + \nu}, \quad \tanh^3 \alpha = a, \quad (112)$$

which describes the charged dipole black ring as a two-soliton solution obtained in Ref. [50]. Further details regarding the solution generation and analysis can be found in the reference. Therefore, we do not explore this case further in this paper.

2. $n = 1$ (a capped black hole with S^3 -horizon topology)

The $n = 1$ case describes a regular solution called a ‘‘capped black hole,’’ characterized by a horizon cross section with a trivial topology of S^3 but the domain of outer communication with a nontrivial topology [79]. In this case, we can show from Eq. (111) that under the condition (83),

$$d_1 = -(1 - \gamma)(1 - \nu)^2 a(2 - a) < 0 \Leftrightarrow 0 < a < 1. \quad (113)$$

For this range of a , Eqs. (81) and (82) can be solved in terms of ν and γ as

$$\nu = 1 - \frac{2b(1 - a^2)^2}{b(2a^2(a - 1)^2 + 1) + a((a - 1)^3 - 1)},$$

$$\gamma = \nu + \frac{(1 - \nu)(1 - a + a^2)}{1 - (1 + 2b)a + (1 + b)a^2}, \quad (114)$$

from which we can show

$$0 < \nu < \gamma < 1 \Leftrightarrow \begin{cases} \frac{a(a-2)(1-a+a^2)}{(1-2a)(1+2a-2a^2)} < b < 0 & (0 < a < a_*) \\ -1 < b < 0 & (a_* \leq a < 1) \end{cases}, \quad (115)$$

where $a_* = 0.347\dots$ is a root of $a^3 - 3a + 1 = 0$. From Eq. (79), this also restricts the range of α to be positive.

From Eq. (114), it is straightforward to show $H(x, y) > 0$ in the coordinate ranges (58) and in the parameter range (115) by writing $H(x, y)$ in the following form [79]:

$$\begin{aligned} H(x, y) = & [\{\nu b^2 c_1^2 (1+\nu)^2 (\gamma-\nu)(1-\gamma)(1-x^2) + \nu(1-\gamma)(\gamma-\nu)(b(1-\nu)^2(1-x) - 2c_1(1+\nu x))^2 \\ & + b^2 c_1^2 (1+\nu)^3 (x+1)(\gamma-\nu)^2\} (1+y)^2] + [\{d_5(1-x)^2 + d_6(1-x^2) + d_7(1+x)(1+\nu x)\}(-1-y)] \\ & + [4(1-a^2)(1-\gamma)^3(1-\nu)^4(1-x) + 2c_2^2(1-\gamma)(1-\nu)^2(1-x^2) - 4d_1(1-\gamma)(1-\nu)^2(1+\nu)(1+x)], \end{aligned} \quad (116)$$

with three extra auxiliary parameters:

$$\begin{aligned} d_5 & := (1-\gamma)(1-\nu)^3 [(\gamma-3\nu)(b^2(\nu-1)(\gamma-\nu) - c_1^2) - 2bc_1(3\nu-1)(\gamma-\nu)], \\ \frac{d_6}{1-\nu} & := \frac{d_7}{2} := c_1(1-\gamma)(1-\nu^2)(c_2 - (1-\gamma)(a-b)(\gamma-\nu)). \end{aligned} \quad (117)$$

It is evident that the first and third square brackets in Eq. (116) are non-negative. It can be shown from Appendix B that d_5 , d_6 , and d_7 in the second square bracket are positive, hence as a result, the second square bracket is also non-negative. Thus, we can show that all three terms enclosed in a square bracket in Eq. (116) are non-negative, and hence $H(x, y)$ is non-negative. Moreover, we can prove a stronger statement, $H(x, y) > 0$, because the three square brackets cannot be zero simultaneously. Having shown $H(x, y) > 0$, we can see that the positivity of D follows from $D = 1 + s^2(H(x, y) - H(y, x))/H(x, y)$ and

$$\begin{aligned} H(x, y) - H(y, x) & = \frac{(1-\nu)(\gamma+\nu)(x-y)}{1+\nu} (c_3(1-\gamma)(1-\nu)^3(1-x)(1-y) \\ & + c_1^2(1+\nu)^2(1+x)(-1-y) + 2(-d_1)(1-\gamma)(1-\nu)[(1+\nu)(1+x) + (1+\nu x)(1-x)]) \geq 0, \end{aligned} \quad (118)$$

where $c_3 > 0$ is obvious from the definition (56).

Moreover, we can demonstrate that this regular solution does not permit the presence of CTCs both on and outside the horizon. To show this explicitly, we need to ensure that the two-dimensional part g_{IJ} (where $I, J = \psi, \phi$) of the metric (73) is positive definite on and outside the horizon, except on the axes at $x = \pm 1$ and $y = -1$, i.e., $\det(g_{IJ}) > 0$ and $\text{tr}(g_{IJ}) > 0$ for $-1 < x < 1$ and $-1/\nu \leq y < -1$. Following the same reasoning as in the case of the charged dipole black ring discussed in Ref. [50], it suffices to demonstrate $\det(g_{IJ}) > 0$ for the ranges $-1 < x < 1$ and $-1/\nu \leq y < -1$. This can be reduced to proving the positivity of $\Delta(x, y)$ defined by

$$\Delta(x, y) := -\frac{(1+\nu x)DH(x, y)}{\ell^4(1-x^2)(1+y)} \det(g_{IJ}). \quad (119)$$

One can easily observe the positivity of this quantity at infinity $(x, y) = (-1, -1)$ since the spacetime approaches the Minkowski metric in that limit. Additionally, around $(x, y) = (1, -1)$, one can show the positivity from the condition $d_1 < 0$, as expressed by

$$\Delta(1, -1) = -4d_1(1-\nu)^3(1+\nu)(1+c^2\nu+s^2\gamma)^3, \quad (120)$$

where we have also used Eq. (79). The positivity on the horizon follows from

$$\Delta(x, -1/\nu) = \frac{4c_3^2(1-\nu)^3(1+\nu)(\gamma+\nu)(c^3(ac_1+\nu-1) - s^3(b-a)(\gamma-\nu))^2}{(1-a^2)^2(1-\gamma)} > 0. \quad (121)$$

For other regions, proving the positivity analytically is challenging. Instead, we have numerically verified the positivity for several values in the parameter region (115) (Fig. 4).

3. $n \geq 2$ (a black lens with $L(n; 1)$ -horizon topology)

For $n \geq 2$, we find $d_1 > 0$ in the range (83), which is contrary to the condition (88). Therefore, at least, within the solution obtained from the seed (50) through the Harrison transformation, this excludes the possibility of a black lens with a horizon cross section of $L(n; 1)$ for $n \geq 2$ as a regular solution not possessing CTCs. However, if we relax the condition (81) and allow for a conical singularity at $x = 1$, we can find parameter ranges without curvature singularities and CTCs, resembling the vacuum case discussed in Ref. [22].

V. CAPPED BLACK HOLE

For $n = 1$, we obtain the spherical black hole in [79] that has a nontrivial DOC in the parameter range (115). In Fig. 5, we illustrate the orbit spaces of our spherical black hole and known spherical black hole (Cvetič-Youm black hole). The inner axis at $x = 1$ for $-1/\nu \leq y \leq -1$ has a disk topology since a S^1 generated by $\partial/\partial\psi$ shrinks to zero at $y = -1$ but not at $y = -1/\nu$. Hence, the horizon is capped by a disk-shaped bubble at a pole and the solution is called the capped black hole. Below, we study the physical properties of the capped black hole.

As one can see from Fig. 3, besides the scale parameter ℓ , the regular solution is characterized by two independent parameters $(\nu, \tanh \alpha) \in (0, 1) \times (0, 1)$. We will see that ν controls the relative size of the disk-shaped bubble and horizon and $\tanh \alpha$ indicates the amount of the electric charge. Note that the metric is no longer Lorentzian on the boundary of the parameter region.

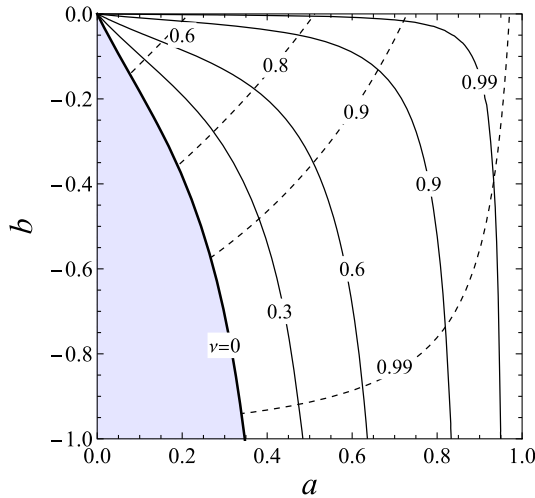


FIG. 3. The parameter region for a regular capped black hole ($n = 1$) given in Eq. (115). The thick and dashed curves correspond to $\nu = \text{constant}$ and $\tanh \alpha = \text{constant}$, respectively. There is no regular black hole in the blue-colored region below $\nu = 0$.

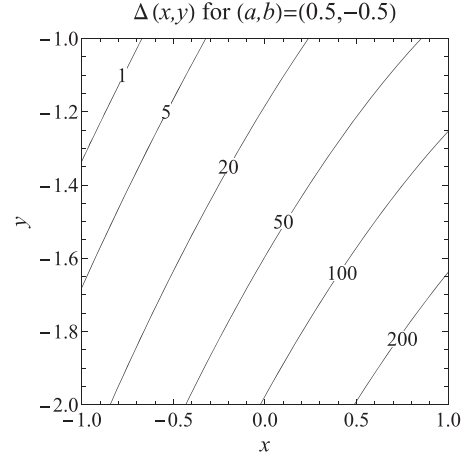


FIG. 4. Profile of $\det(g_{IJ})$ for parameters given by Eqs. (79) and (114) with $(a, b) = (0.5, -0.5)$. One can obtain similar profiles for other sets of (a, b) in the range (115).

A. Physical quantities

As shown previously in Eq. (85), the spacetime is asymptotically flat, and hence the Arnowitt-Deser-Misner (ADM) mass M and two ADM angular momenta J_ψ, J_ϕ can be read off from the asymptotic of the metric at $r \rightarrow \infty$ in the coordinates (84),

$$\begin{aligned}
 ds^2 = & - \left(1 - \frac{8G_5 M}{3\pi r^2} \right) dt^2 - \frac{8G_5 J_\psi \sin^2 \theta}{\pi r^2} dt d\psi \\
 & - \frac{8G_5 J_\phi \cos^2 \theta}{\pi r^2} dt d\phi + dr^2 + r^2 \sin^2 \theta d\psi^2 \\
 & + r^2 \cos^2 \theta d\phi^2 + r^2 d\theta^2, \tag{122}
 \end{aligned}$$

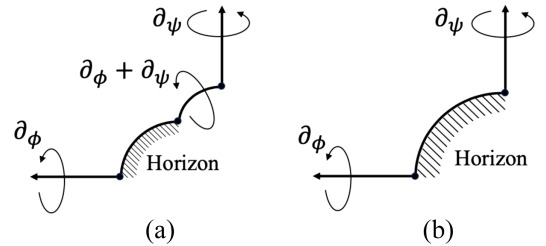


FIG. 5. The orbit space $\mathcal{M}^{(1,4)}/[\mathbb{R} \times U(1) \times U(1)]$ of (a) the capped black hole and (b) the Cvetič-Youm black hole. In each panel, the bold curves—excluding the event horizon—represent the rotational axes, which serve as fixed points for the action of the $U(1)$ isometries along the corresponding Killing vector fields. The intersection of a rotational axis with a horizon denotes a set of fixed points for the $U(1)$ action, forming the topology of a circle in a given time slice. In panel (a), the intersection of two distinct rotational axes, associated with the fixed points of the $U(1)$ actions along the Killing vector fields $\partial_\phi + \partial_\psi$ and ∂_ϕ , constitutes a common fixed point for the two different $U(1)$ actions, which topologically is a point.

with

$$M = \frac{3\pi\ell^2(1+2s^2)(\gamma+\nu)(c_3(1-\nu)-d_1)}{4G_5(1-a^2)(1-\gamma)^2(1+\nu)}, \quad (123)$$

$$J_\psi = c^3 J_1 + s^3 J_2, \quad (124)$$

$$J_\phi = c^3 J_2 + s^3 J_1, \quad (125)$$

where J_1 and J_2 correspond to the angular momenta in the neutral case around the ψ -rotational axis and ϕ -rotational axis, respectively, given by

$$J_1 = \frac{\pi\ell^3 v_0(c_3 d_2 - c_1 c_2 c_3 - (c_3 - b c_2) d_1)}{4G_5(1-a^2)(1-\gamma)^3 \nu}, \quad (126)$$

$$J_2 = \frac{\pi\ell^3 v_0(a-b)(2c_3 \nu + d_1)}{2G_5(1-a^2)(1-\gamma)(1+\nu)}. \quad (127)$$

Additionally, the electric charge is defined by the integration over a three-dimensional closed surface S surrounding a horizon and a bubble or spatial infinity S_∞ :

$$\begin{aligned} Q &:= \frac{1}{8\pi G_5} \int_S \left(\star F + \frac{1}{\sqrt{3}} F \wedge A \right) \\ &= \frac{1}{8\pi G_5} \int_{S_\infty} \star F \\ &= -\frac{2 \tanh \alpha}{\sqrt{3}} M, \end{aligned} \quad (128)$$

where in the second equality, we have used the fact that the Chern-Simons term falls much faster at the asymptotic limit. This obviously follows the Bogomol'nyi bound $M \geq \frac{\sqrt{3}}{2} |Q|$, which is saturated at the limit $\alpha \rightarrow \infty$.

It is worth emphasizing that the electric charge evaluated over the three-dimensional surface S_∞ at infinity does not coincide with one evaluated over the spatial cross section of the horizon $S_{\mathcal{H}}$. The rest of the contribution comes from the three-dimensional surface surrounding the disk-shaped bubble \mathcal{D} . By direct computation, one can confirm that

$$\begin{aligned} Q &:= \frac{1}{8\pi G_5} \int_{S_\infty} \left(\star F + \frac{1}{\sqrt{3}} F \wedge A \right) \\ &= \frac{1}{8\pi G_5} \int_{S_{\mathcal{H}}} \left(\star F + \frac{1}{\sqrt{3}} F \wedge A \right) \\ &\quad + \frac{1}{8\pi G_5} \int_{\mathcal{D}_{\epsilon \rightarrow 0}} \left(\star F + \frac{1}{\sqrt{3}} F \wedge A \right), \end{aligned} \quad (129)$$

$$\quad (130)$$

where \mathcal{D}_ϵ denotes the three-dimensional surface at $x = 1 - \epsilon$ for $-1/\nu \leq y \leq -1$. This is same as the electric charge for the charged dipole black ring [50].

In addition to these conserved charges, one can define the magnetic flux (this is not a conserved charge) over the disk-shaped bubble \mathcal{D} at $x = 1$ as

$$\begin{aligned} q &:= \frac{1}{4\pi} \int_{\mathcal{D}} F = \frac{1}{2} A_\psi(x=1, y=-1/\nu) \\ &= \frac{\sqrt{3} \ell s c d_1 v_0 (b d_2 s (\gamma - \nu) - 2 c \nu \tilde{d}_2)}{2(c^2 d_2^2 (\gamma - \nu) + 2 \nu s^2 \tilde{d}_2^2)}. \end{aligned} \quad (131)$$

where $\tilde{d}_2 := d_2 - (\gamma - 1)(\nu - 1)(\gamma + \nu)$. The area of a constant time slice through the horizon is written as

$$A_H = 8\pi^2 \ell^2 \nu \kappa^{-1}, \quad (132)$$

where the surface gravity κ is given by Eq. (97).

In Ref. [81], it is shown that the black hole with a disk-shaped bubble must follow the first law

$$\delta M = \frac{\kappa}{8\pi} \delta A_H + V_\psi \delta J_\psi + V_\phi \delta J_\phi + \frac{1}{2} \Phi_H \delta Q + \mathcal{Q}_{\mathcal{D}} \delta \Phi_{\mathcal{D}}, \quad (133)$$

and the Smarr formula

$$M = \frac{3\kappa A_H}{16\pi} + \frac{3}{2} V_\psi J_\psi + \frac{3}{2} V_\phi J_\phi + \frac{1}{2} \Phi_H Q + \frac{1}{2} \mathcal{Q}_{\mathcal{D}} \Phi_{\mathcal{D}}, \quad (134)$$

where Φ_H is the electric potential (104), $\Phi_{\mathcal{D}}$ and $\mathcal{Q}_{\mathcal{D}}$ are the magnetic potential and another type of a magnetic flux on the bubble \mathcal{D} , which are defined as

$$\begin{aligned} \Phi_{\mathcal{D}} &:= -(A_\phi + n A_\psi)|_{x=1} \\ &= -\sqrt{3} c s \ell v_0 (c(a-b) - s(1-ab)), \end{aligned} \quad (135)$$

$$\begin{aligned} \mathcal{Q}_{\mathcal{D}} &:= \frac{1}{4} \int_{\mathcal{D}} \left[l_{v_H} (\star F) - \frac{1}{\sqrt{3}} (\Phi - \Phi_H) F \right] \\ &= \frac{\sqrt{3} \pi (1-a^2) b c d_1 \ell s v_0}{4c_3 (c^3 (a c_1 + \nu - 1) - s^3 (b-a)(\gamma - \nu))}. \end{aligned} \quad (136)$$

As depicted in Fig. 6, the two magnetic fluxes q and $\mathcal{Q}_{\mathcal{D}}$ differ in general. Specifically, q can vanish even with the existence of the bubble, while $\mathcal{Q}_{\mathcal{D}}$ is negative definite. When considering the horizon velocities in Eq. (98), one can verify that the capped black hole adheres to the aforementioned first law and Smarr formula by expressing each variable as a function of (ℓ, a, b) using Eqs. (79) and (114).

To discuss the phase space of the capped black hole, let us introduce the angular momenta and horizon area normalized by the mass scale $r_M := \sqrt{8G_5 M / 3\pi}$ as

$$j_\psi := \frac{4G_5}{\pi r_M^3} J_\psi, \quad j_\phi := \frac{4G_5}{\pi r_M^3} J_\phi, \quad a_H := \frac{\sqrt{2}}{\pi^2 r_M^3} A_H. \quad (137)$$

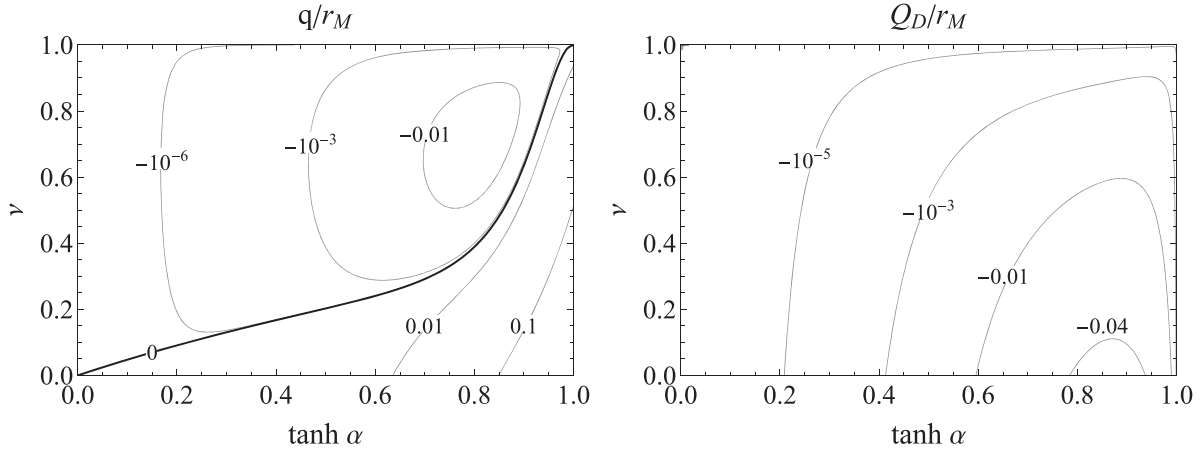
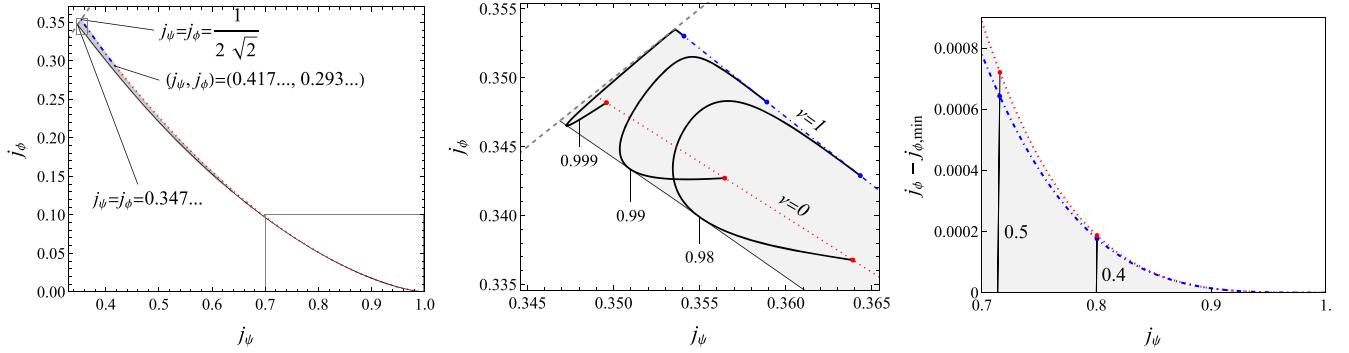

 FIG. 6. Profiles for magnetic fluxes q and Q_D in the $(\nu, \tanh \alpha)$ plane.


FIG. 7. The allowed region for j_ψ and j_ϕ and curves of constant $\tanh \alpha$ are displayed in the (j_ψ, j_ϕ) plane. The allowed region is illustrated by the colored region. Each curve of constant $\tanh \alpha$ starts at the $\nu = 0$ curve (blue dot-dashed) and ends at the $\nu = 1$ curve (red dotted). In the middle panel, we show a closeup of the phases for $\tanh \alpha \approx 1$. At the limit $\alpha \rightarrow 0$, the curves of constant $\tanh \alpha = \text{const}$ converge around $(j_\psi, j_\phi) = (1, 0)$, and the allowed region exists in a very narrow range. From the right panel, one can observe that this range becomes narrower and narrower as j_ψ approaches 1. The plot depicts two angular momenta and several curves of constant $\tanh \alpha$ accompanied by the value of $\tanh \alpha$.

Figure 7 provides insight into the allowed region for the angular momenta in the (j_ψ, j_ϕ) plane. This figure reveals several important physical characteristics of the capped black hole:

- (i) The allowed range for angular momenta is constrained such that $0 < j_\phi < 1/(2\sqrt{2}) \approx 0.353\dots$ and $0.347\dots < j_\psi < 1$. Compared to the Cvetič-Youm black hole [82], this region is notably narrower.
- (ii) The solid curves represent different values of $\tanh \alpha$ (the electric charge), with each curve having endpoints at $\nu = 0$ and $\nu = 1$.
- (iii) The allowed region is bounded by the dashed line $j_\psi = j_\phi$, which can only be reached at the BPS limit $M = \sqrt{3}|Q|/2$ as $\alpha \rightarrow \infty$. However, it is important

to note that the metric is not Lorentzian at the BPS limit. Therefore, the capped black hole does not admit equal angular momenta $j_\psi = j_\phi$.

- (iv) Since each $\tanh \alpha = \text{const}$ curve, as seen in the middle panel, is not closed, the capped black hole is uniquely specified by the conserved charges of its mass, two angular momenta, and electric charge. This implies that there is no continuous family of solutions parametrized by the magnetic flux q , highlighting the uniqueness of the capped black hole configuration.

B. Nonuniqueness of spherical black holes

Now, we compare the capped black hole with the Cvetič-Youm black hole [33,82] having the same conserved

charges, the mass, angular momenta, and electric charge. The normalized angular momenta and the normalized horizon area for the Cvetič-Youm solution are give by, respectively,

$$j_{\psi}^{\text{CY}} = \frac{c^3 j_1 + s^3 j_2}{(1 + 2s^2)^{\frac{3}{2}}}, \quad j_{\phi}^{\text{CY}} = \frac{c^3 j_2 + s^3 j_1}{(1 + 2s^2)^{\frac{3}{2}}}, \quad a_H^{\text{CY}} = \frac{\sqrt{2}[\sqrt{1 - (j_1 + j_2)^2}(c^3 + s^3) + \sqrt{1 - (j_1 - j_2)^2}(c^3 - s^3)]}{(1 + 2s^2)^{\frac{3}{2}}}, \quad (138)$$

where α in $(c, s) = (\cosh \alpha, \sinh \alpha)$ is the same parameter as in the capped black hole, and j_1, j_2 are the dimensionless parameters for the angular momenta. To match the angular momenta of the Cvetič-Youm black hole with those of the capped black hole in Eq. (137), we set

$$j_1 = (1 + 2s^2)^{3/2} \frac{4G_5 J_1}{\pi r_M^3}, \quad j_2 = (1 + 2s^2)^{3/2} \frac{4G_5 J_2}{\pi r_M^3}. \quad (139)$$

Here we note that the Cvetič-Youm black hole reaches the extremal limit, which does not coincide with the BPS limit when $|j_1 + j_2| = 1$ or $|j_1 - j_2| = 1$ [82]. Hence, the

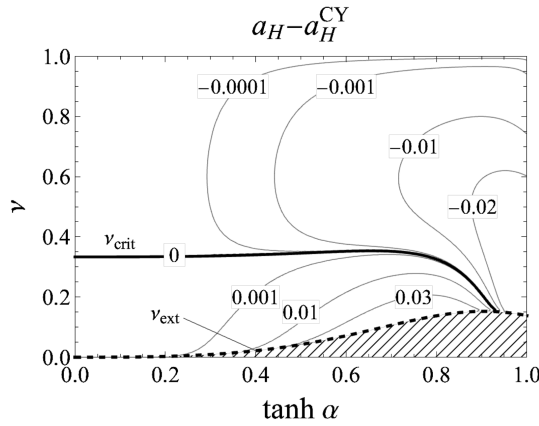


FIG. 8. The area of the horizon cross section of the capped black hole compared with that of the Cvetič-Youm black hole of the same (j_{ψ}, j_{ϕ}) in the $(\nu, \tanh \alpha)$.

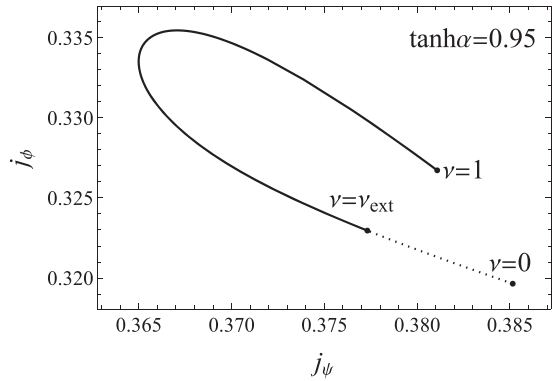
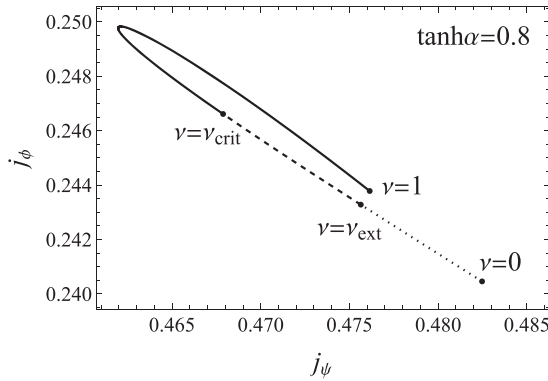


FIG. 9. The area of the horizon cross section of the capped black hole compared with that of the Cvetič-Youm black hole on the contour in (j_{ψ}, j_{ϕ}) plane for some fixed α ($\tanh \alpha = 0.8, 0.95$). The Cvetič-Youm black hole is favored on the thick curve, while ours is favored on the dashed. On the dotted curve, the Cvetič-Youm black hole does not exist.

Cvetič-Youm black hole cannot match the capped black hole if j_1 and j_2 in Eq. (139) exceed the bound $|j_1 + j_2| \leq 1$ or $|j_1 - j_2| \leq 1$.

Here are the observations from Fig. 8 regarding the difference in the horizon area of the two phases in the $(\nu, \tanh \alpha)$ -plane:

- For a fixed α , the corresponding Cvetič-Youm black hole becomes extremal at $\nu = \nu_{\text{ext}}(\alpha)$ for $|j_1 + j_2| = 0$, and has the same horizon area at $\nu = \nu_{\text{crit}}(\alpha)$.
- For $0 < \nu < \nu_{\text{ext}}(\alpha)$ (the shaded region) and a fixed α , there is no Cvetič-Youm black hole corresponding to the capped black hole with the same angular momenta because of $|j_1 + j_2| > 1$,
- For $\nu_{\text{ext}}(\alpha) < \nu < \nu_{\text{crit}}(\alpha)$ and a fixed α ($\tanh \alpha < 0.940\dots$), the capped black hole has larger entropy and hence is thermodynamically more stable than the Cvetič-Youm black hole, and for $\nu > \nu_{\text{crit}}(\alpha)$, on the other hand, the Cvetič-Youm black hole is more stable.

As depicted in Fig. 9, for $\tanh \alpha < 0.940\dots$, each curve of constant $\tanh \alpha$ can be segmented into three parts: (i) $0 < \nu < \nu_{\text{ext}}(\alpha)$, (ii) $\nu_{\text{ext}}(\alpha) < \nu < \nu_{\text{crit}}(\alpha)$, and (iii) $\nu_{\text{crit}}(\alpha) < \nu < 1$, while for $\tanh \alpha > 0.940\dots$, there are only two segments without the range $\nu_{\text{ext}}(\alpha) < \nu < \nu_{\text{crit}}(\alpha)$.

C. Size of horizon and bubble

As one might expect from the rod structure depicted in Fig. 2, the parameter ν indicates the size of the bubble, with smaller values of ν indicating larger bubbles. The horizon disappears as ν approaches 0, while the bubble disappears as ν tends to 1. To illustrate this characteristic, we introduce

two scales that represent the sizes of the horizon and the bubble. Analogous to the horizon area, one can calculate the two-dimensional area of the bubble as

$$a_D := \frac{A_D}{\pi r_M^2} = \frac{2}{r_M^2} \int_{-1/\nu}^{-1} \sqrt{g_{yy}g_{\psi\psi}}|_{x=1} dy, \quad (140)$$

where a_D is the mass-normalized bubble area. As shown in the top panels of Fig. 10, the horizon area vanishes as $\nu \rightarrow 0$, while the bubble area remains finite. Although both areas vanish as $\nu \rightarrow 1$, a comparison of the area scales defined by $\ell_H := a_H^{1/3}$ and $\ell_D := a_D^{1/2}$ reveals that the bubble scale decreases more rapidly, with $\ell_H/\ell_D \sim (1-\nu)^{-1/3}$ (see also the bottom left panel in Fig. 10).

To investigate the distortion of the S^3 horizon, we also compare R_{\pm} defined in Eqs. (107) and (108), which estimate the radial scales of the horizon at each pole. From the bottom right panel of Fig. 10, it is evident that the ratio between R_+ and R_- remains finite even as $\nu \rightarrow 1$, indicating that the horizon shape does not collapse in the limit. If the electric charge is sufficiently small, we observe $R_+/R_- \rightarrow 0$, suggesting that the horizon shape becomes elongated along the ψ -rotation plane.

D. Ergoregion

The ergoregion of the capped black hole (50) is determined by the condition $H(y, x) < 0$. To comprehend the presence of the ergoregion, it is convenient to use the

following properties for the parameters within the range (115) together with Eq. (114) (refer to Appendix C for the proof):

- (a) $H(y = -1, x = \pm 1) > 0$,
 - (b) $H(y = -1/\nu, x) < 0$ for $x \in [-1, 1]$,
 - (c) $\partial_x^2 H(y = -1, x) > 0$ for $x \in [-1, 1]$,
 - (d) $\partial_y^2 H(y, x) < 0$ for $(x, y) \in [-1, 1] \times [-1/\nu, -1]$,
 - (e) $\partial_y H(y = -1, x) + H(y = -1, x) > 0$ for $x \in [-1, 1]$.
- (a) indicates that both the asymptotic infinity and the intersection of the inner rotational axis and the ψ -rotational axis always lie outside the ergoregion, while (b) illustrates that the horizon is invariably situated inside the ergoregion. (c) demonstrates that $H(y = -1, x)$ is a concave function of x , which, combined with (a), leads to the following two potential behaviors on the ψ -rotational axis at $y = -1$:
- (i) $H(y = -1, x) > 0$ for $x \in [-1, 1]$,
 - (ii) $H(y = -1, x) > 0$ for $x \in [-1, x_1] \cup (x_2, 1]$ and $H(y = -1, x) < 0$ for $x \in (x_1, x_2)$,

where x_1 and x_2 are certain constants such that $-1 < x_1 < x_2 < 1$. Moreover, (d) and (e) ensure that for a given $x \in [-1, 1]$:

- (i) $H(y, x) = 0$ has a single root for $y \in (-1/\nu, -1]$ if $H(y = -1, x) \geq 0$,
- (ii) $\partial_y H(y = -1, x) = -H(y = -1, x) > 0$ and then $H(y, x)$ is a monotonically increasing function of y if $H(y = -1, x) < 0$,

which excludes the case where $H(y, x) > 0$ for $\exists y \in (-1/\nu, -1)$ but $H(y = -1, x) < 0$ and $H(y = -1/\nu, x) < 0$. Therefore, we find that the capped black hole admits two

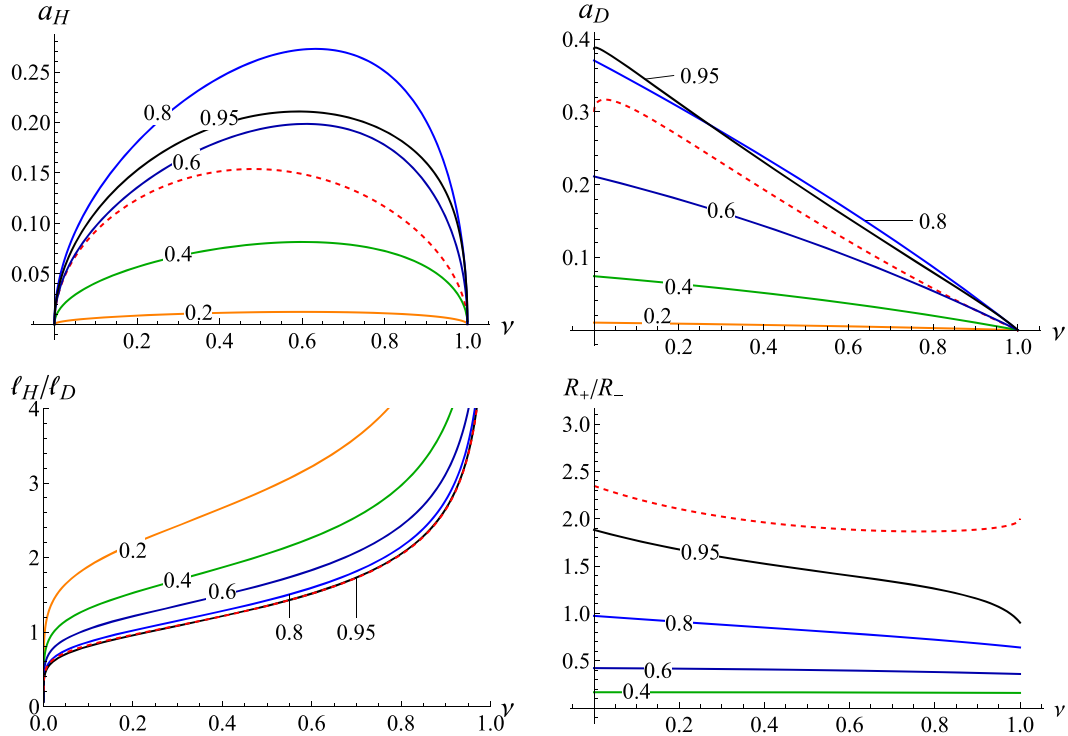


FIG. 10. ν dependence of horizon and bubble scales for each $\tanh \alpha$. The value of $\tanh \alpha$ is shown with each curve. The red dashed curves correspond to the limit curve at $\tanh \alpha \rightarrow 1$.

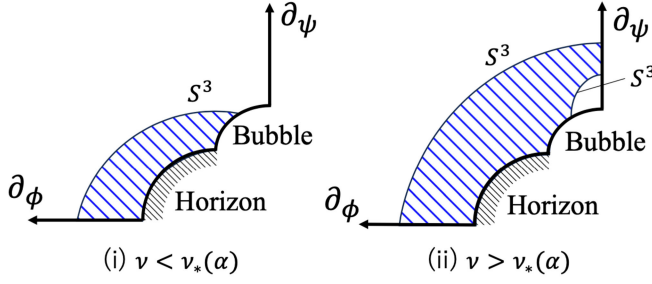


FIG. 11. Possible shapes for the ergoregion: The ergoregions are illustrated by the blue hatched pattern in the orbit space for two cases, (a) $\nu < \nu_*(\alpha)$ and (b) $\nu > \nu_*(\alpha)$.

types of ergosurfaces, whose topology changes across a value $\nu = \nu_*(\alpha)$ where a quadratic function $H(y = -1, x)$ exhibits a double root within the range $-1 \leq x \leq 1$ (Fig. 11):

- (i) $0 < \nu < \nu_*(\alpha)$: a single S^3 surface around the horizon,
- (ii) $\nu_*(\alpha) < \nu < 1$: an outer S^3 surface that encompasses both the horizon and bubble, and an inner S^3 surface around the flat center at $(x, y) = (1, -1)$.

In case (ii), the ergoregion extends to the rotation axis of ψ , while the ball region around the center at $(x, y) = (1, -1)$ is excluded from the ergoregion due to being the fixed point of two rotations. In Fig. 12, we illustrate the threshold curve $\nu = \nu_*(\alpha)$ and the topology of the ergosurface in the phase diagram.

One might understand the topology change of the ergoregion from the change in the bubble size discussed in the previous section. For small enough ν , the bubble is sufficiently large compared to the horizon scale, and hence it protrudes out of the ergoregion as in case (i). As ν increases, the bubble becomes smaller, and for $\nu = \nu_*(\alpha)$, it is completely engulfed by the ergoregion. The inner ergosurface exists for $\nu_*(\alpha) \leq \nu < 1$, but it vanishes as ν approaches 1, since the bubble shrinks to a point in the limit and the spacetime approaches the extremal (non-BPS) Cvetič-Youm black hole. Note that in both cases, there does not exist a so-called evanescent ergosurface,

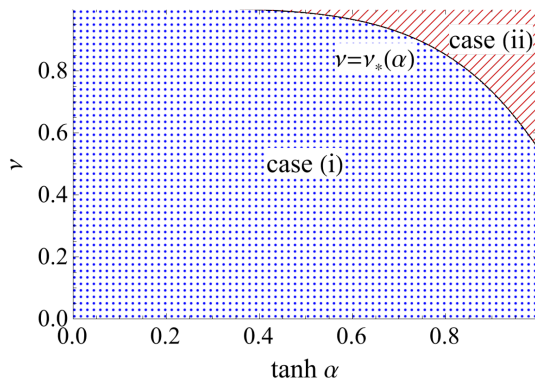


FIG. 12. The topology change of the ergoregion in the phase diagram.

which is a timelike surface outside the horizon where the timelike Killing vector field at infinity becomes null on the surface but remains timelike both inside and outside the surface [30].

VI. SUMMARY AND DISCUSSION

In this paper, applying the electric Harrison transformation to the vacuum black lens solutions possessing a Dirac-Misner string singularity, we have constructed asymptotically flat, stationary, biaxially symmetric black hole solutions within the bosonic sector of five-dimensional minimal supergravity. Initially, we have obtained the vacuum black lens solutions, which inherently contained Dirac-Misner string singularities, using the inverse scattering method. Then, by implementing the Harrison transformation on the vacuum solution, we successfully eliminated the Dirac-Misner string singularities by appropriately adjusting the parameters involved. The resulting black hole solutions exhibit horizon topologies of lens space $L(n; 1)$, including the $n = 0$ and $n = 1$ cases. It has been demonstrated that these black hole solutions are singular for $n \geq 2$, but regular for $n = 0, 1$. The $n = 0$ case describes the charged rotating black ring with a dipole charge constructed in Ref. [50], and the $n = 1$ case describes the capped black hole constructed in Ref. [79]. In particular, the $n = 1$ case is interesting because this solution describes an asymptotically flat, stationary, non-BPS black hole with a horizon cross section of trivial topology S^3 , while the domain of outer communication (DOC) exhibits a nontrivial topology. This solution remains regular without any curvature singularities, conical singularities, Dirac-Misner string singularities, and orbifold singularities both on and outside the horizon. It describes a charged rotating black hole capped by a disk-shaped bubble, which we call a capped black hole. We have demonstrated that the spherical black hole carries mass, two angular momenta, an electric charge, and a magnetic flux, where only three of these quantities are independent. Moreover, we have shown that this black hole can have identical conserved charges as the spherical black hole found by Cvetič-Youm, thus indicating a violation of black hole uniqueness even when assuming that the topology of the horizon cross section is S^3 . Additionally, we have found that the capped black hole can possess larger entropy compared to the Cvetič-Youm black hole, establishing the spherical black hole with a significant bubble as thermodynamically more stable.

We would like to comment on the intersection of the horizon $\partial\Sigma_{\mathcal{H}} = \{(x, y) | y = -1/\nu, -1 \leq x \leq 1\}$ and the bubble $\partial\Sigma_{\text{in}} = \{(x, y) | x = 1, -1/\nu \leq y \leq -1\}$. Each point on $\{(x, y) | x = 1, -1/\nu < y < -1\}$, a fixed point of the Killing vector v_ψ , corresponds to a circle generated by another Killing vector v_ϕ . Furthermore, v_ψ vanishes at $(x, y) = (1, -1)$ but does not vanish at $(x, y) = (1, -1/\nu)$.

Consequently, since $\partial\Sigma_{\text{in}}$ is topologically D^2 , this two-dimensional disk-shaped bubble intersects with the horizon at the one-dimensional circle $(x, y) = (1, -1/\nu)$. Therefore, the horizon appears to be capped by the disk-shaped bubble. However, it should be noted that the term ‘‘capped’’ does not imply that a part of the S^3 horizon is cut out and replaced with another structure; rather, the horizon itself truly is S^3 . This can be seen as follows: Each point on $\{(x, y)|y = -1/\nu, -1 < x < 1\}$ represents a two-dimensional torus generated by the two Killing vectors, $v_\phi := \partial_\phi = (0, 1)^T$ and $v_{\phi'} := \partial_{\phi'} = \partial_\psi + \partial_\phi = (1, 1)^T$. Moreover, since these vectors vanish at the endpoints $x = -1$ and $x = 1$, respectively, the endpoints $(x, y) = (-1, -1/\nu)$ and $(x, y) = (1, -1/\nu)$ form circles generated by v_ϕ and $v_{\phi'}$, respectively. Therefore, since the segment $\partial\Sigma_{\mathcal{H}} = \{(x, y)|y = -1/\nu, -1 \leq x \leq 1\}$ can be regarded as the union of two solid tori, along with $\det(v_\phi, v_{\phi'}) = -1$, it turns out that $\partial\Sigma_{\mathcal{H}}$ is actually S^3 . Hence, a part of the S^3 horizon is not cut out by the bubble rather, the horizon itself is complete S^3 .

The topology of the DOC on a timeslice Σ can easily be read off from the rod structure, as described in Ref. [35]. According to the topology censorship theorem [34], the intersection $X = \text{DOC} \cap \Sigma$ in an asymptotically flat space-time must be simply connected. Therefore, in a biaxisymmetric spacetime, the orbit space $\hat{X} = X/U(1)^2$ reduced to two dimensions by two $U(1)$ isometries is also simply connected. This results in the rod diagram representing the upper half-plane in \mathbb{R}^2 , as depicted in Fig. 13. For simplicity, we assign only the spacial components of the rod vector to each rod, and the rod vectors on the semi-infinite rods are set to be $(0, 1)^T$ and $(1, 0)^T$, respectively. Note that, to match the orientation in Ref. [35], we assign the rod vector $m_\phi \partial_\phi + m_\psi \partial_\psi$ to $(m_\phi, m_\psi)^T$ so that the semi-infinite rod with $(1, 0)^T$ corresponds to the left side. Following the procedure in Ref. [35], to know the

topological structure of $X = \text{DOC} \cap \Sigma$ on a timeslice Σ for the capped black hole, let us consider a sufficiently large outer sphere S_{out} and a sphere S_{in} sufficiently close to the horizon, which divide X into three regions: the asymptotic region X_{out} outside S_{out} , including spatial infinity, the inner region X_{in} between S_{out} and S_{in} , and the near-horizon region X_{H} between S_{in} and the horizon. We denote the corresponding counterparts in the orbit space with hats. As depicted in Fig. 13, the curve \hat{S}_{out} , represented by the blue dashed curve, terminates at the two rods with $(1, 0)^T$ and $(0, 1)^T$, and the curve \hat{S}_{in} , represented by the red dotted curve, terminates at the two rods with $(1, 0)^T$ and $(1, 1)^T$, where as shown Ref. [17], it is ensured from the orientations of these rod vectors that S_{out} and S_{in} are topologically S^3 . The procedure in Ref. [35] is as follows: (i) First, by gluing \hat{X}_{out} and a half-disk \hat{D}_{out} , which is such that $D_{\text{out}} \cong \mathbb{B}^4$, along a semicircle \hat{S}_{out} , one can obtain an upper half-plane [in other words, by gluing X_{out} and D_{out} along S_{out} , one can obtain \mathbb{R}^4], (ii) next, by gluing a half-disk \hat{D}'_{out} ($D'_{\text{out}} \cong \mathbb{B}^4$) along a semicircle \hat{S}_{out} , and (iii) finally, by gluing another half-disk \hat{D}_{in} ($D_{\text{in}} \cong \mathbb{B}^4$) along a semicircle \hat{S}_{in} , one can obtain a compact two-dimensional space bounded by a closed curve with three endpoints (similarly, by gluing D'_{out} along S_{out} and D_{in} along S_{in} to X_{in} , one can obtain a compact, simply connected four-manifold). According to the classification in Ref. [83], the topology of the four-dimensional space with this type of rod diagram turns out to be $\mathbb{C}\mathbb{P}^2$. Thus, we find $X_{\text{out}} \cup X_{\text{in}} \cup D_{\text{in}} \cong \mathbb{R}^4 \# \mathbb{C}\mathbb{P}^2$. Since $X \cong X_{\text{out}} \cup X_{\text{in}}$, we can conclude that the capped black hole constructed in this paper has the DOC such that $\text{DOC} \cap \Sigma \cong [\mathbb{R}^4 \# \mathbb{C}\mathbb{P}^2] \setminus \mathbb{B}^4$.

The capped black hole derived in this paper is characterized by four conserved charges: the mass, two angular momenta, and an electric charge, along with a magnetic flux. However, these quantities are not all independent. It is expected that there may exist a more general capped black

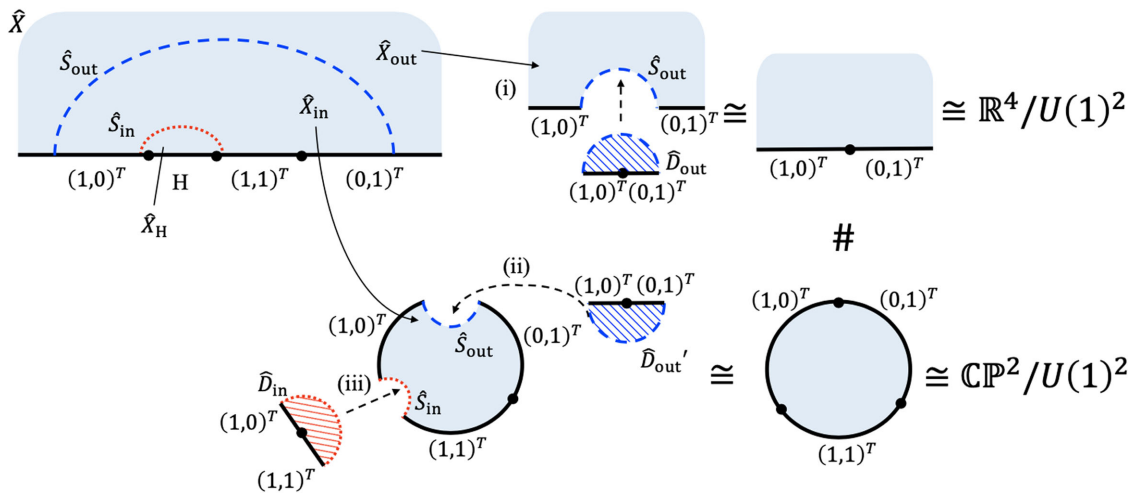


FIG. 13. The topology of the DOC can be seen from the rod diagram.

hole with five independent quantities. The construction of such a solution deserves further investigation. Additionally, so far, an exact solution of a non-BPS black lens, even a vacuum solution, has not been found. In this paper, we also attempted the construction of black lenses applying the electric Harrison transformation on the Chen-Teo type configuration as described in Ref. [22]. However, though we could obtain the capped black hole solution and charged dipole black ring solution as a by-product, our work does not yield any regular solutions for black lenses. Exploring this avenue is part of our future work. It is conceivable that applying the Harrison transformation to the four-soliton solution referenced in Ref. [23] might enable us to uncover a regular charged black lens solution. Recently, a regular static black lens immersed in the external magnetic field—which is not asymptotically flat—was produced by combining the Harrison transformation and another type of

transformation in the context of the five-dimensional Einstein-Maxwell theory [84]. Hence, the presence of the magnetic field plays a significant role in the support of a black lens horizon, as suggested previously for supersymmetric black lenses [30]. In our forthcoming paper, we will discuss another construction of a non-BPS charged black lens solution in five-dimensional minimal supergravity.

ACKNOWLEDGMENTS

The authors are grateful to Marcus Khuri for useful comments and discussion on the topology of the DOC during the 32nd workshop on General Relativity and Gravitation in Japan (JGRG32). R. S. was supported by JSPS KAKENHI Grant No. JP18K13541. S. T. was supported by JSPS KAKENHI Grant No. 21K03560.

APPENDIX A: COEFFICIENTS FOR $K(x,y)$

The coefficients in Eq. (65) are given by

$$\begin{aligned}
 k_1 &= 2c_1c_2c_3\nu(\nu+1)(a-b)(\gamma-\nu), & k_2 &= -c_2(1-\nu)(a-b)(\gamma-\nu)(c_1c_3-bd_1), \\
 k_3 &= \frac{c_2d_1(1-\nu)(\gamma c_3 - c_3\nu - d_2)}{(1-\gamma)(\nu+1)}, & k_4 &= \frac{(1-\gamma)^3c_2c_3(1-\nu)^2((1-\gamma)(1-\nu)(\gamma+\nu) + d_1 - d_2)}{(1-\gamma)^4(\nu+1)}, \\
 k_5 &= 2c_3d_3(1-\nu)^3(\gamma-\nu), & k_6 &= \frac{c_2c_3(\gamma^2(\nu-1)^2 + \gamma((\nu-1)^3 - 2d_1) - (\nu-1)(d_2 + (\nu-1)\nu) + d_1(3\nu-1))}{(1-\gamma)(1+\nu)}, \\
 k_7 &= -\frac{8d_1[(1-\gamma)(1-\nu)^2(\gamma-\nu)(b(\nu-1) + c_1) + 2c_1c_3(\gamma-\nu) - c_1d_2(1-\nu)]}{(1-\gamma)(\nu+1)}.
 \end{aligned} \tag{A1}$$

APPENDIX B: PROOF OF $H(x,y) > 0$ AND $D > 0$ FOR $n=1$

Here we show the positivity of each term in Eq. (116). With the negativity of d_1 (88), it suffices to show the positivity of d_5, d_6, d_7 defined in Eq. (117). For this, it is convenient to clarify the signature of c_1 by rewriting it with Eqs. (82) and (81) as

$$c_1 = -(1-\gamma)^2(1-d)^2(-d_1)^{-1}(1-a)(1-a^2) < 0. \tag{B1}$$

This also imply $c_2 < 0$ due to the identity

$$c_2 = c_1(1+\nu) - (1-\gamma)(1-\nu)a < 0. \tag{B2}$$

With $c_1, c_2 < 0$, the positivity of d_6 and d_7 is obvious from the definition. The positivity of d_5 is a little less trivial. First, we consider the following quantity:

$$\begin{aligned}
 \tilde{d}_5 &= \frac{ab^2(2-a)(1-a^2)^2}{(1-\gamma)^4(1-\nu)^3} d_5 = (2-a)a^3(a^2-a+1)^2 + b(a^2-a+1)(8a^5 - 13a^4 + 2a^3 - a^2 + 2a - 1) \\
 &\quad + ab^2(2a^6 - 14a^5 + 22a^4 - 17a^3 + 16a^2 - 8a + 2) + (2a-1)b^3(a^2-a+1)(2a^2-2a-1),
 \end{aligned} \tag{B3}$$

where we used Eq. (114). One can see the positivity of d_5 by writing \tilde{d}_5 as the sum of positive definite terms

$$\begin{aligned} \tilde{d}_5 = & (2-a)^3 a^3 (1-a+a^2)^2 (1+b^3) + (-b)(1-b^2)(1-a+a^2) \left[\frac{5}{18} + \frac{1}{2}(1-a)^4 + \frac{9}{2} \left(a^2 - \frac{2}{9} \right)^2 + 8a^4(1-a) \right] \\ & + b^2(1+b)a \left[2(1-a)^4 + 6a^2 \left(a - \frac{3}{4} \right)^2 + \frac{5}{8}a^2 + 2a^6 + 14a^4(1-a) \right] + (-b)^3 a^2 (1+a)^3 (1+a^2-a^3) > 0. \end{aligned} \quad (\text{B4})$$

APPENDIX C: PROPERTIES OF $H(y,x)$ FOR $n=1$

Here we prove several properties of $H(y,x)$ that are used to determine the topology of the ergoregion for the capped black hole in Sec. V D. We use the following conditions proved in Sec. IV C and Appendix. B

$$d_1 < 0, \quad c_1 < 0, \quad c_3 > 0. \quad (\text{C1})$$

- (1) Proof of (a) $H(y=-1, x=\pm 1) > 0$ and (c) $\partial_x^2 H(y=-1, x) > 0$ for $x \in [-1, 1]$.

These can be shown directly from

$$H(y=-1, x=1) = -8(1-\gamma)^2 d_1 (1-\nu)^2 > 0, \quad (\text{C2})$$

$$H(y=-1, x=-1) = 8(1-\gamma)^3 (1-\nu)^4 (1-a^2) > 0, \quad (\text{C3})$$

$$\partial_x^2 H(y=-1, x) = 8\nu(1-\gamma)^3 (\gamma-\nu)(1-\nu)^2 (a-b)^2 > 0. \quad (\text{C4})$$

- (2) Proof of (b) $H(y=-1/\nu, x) < 0$ for $x \in [-1, 1]$.

The negativity of $H(y=-1/\nu, x)$ is obvious by writing it as

$$H(y=-1/\nu, x) = A_1(1+x)^2 + A_2(1-x)^2 + A_3(1-x^2), \quad (\text{C5})$$

where

$$A_1 = \frac{(1-\nu)^2(1+\nu)(c_2 - (1-\nu)(1-\gamma)(\gamma+\nu))^2}{\nu(\gamma-\nu)} > 0, \quad (\text{C6})$$

$$A_2 = \frac{(1-\gamma)c_3(\gamma-\nu)(1-\nu)^4(1+\nu)}{2\nu^2} > 0, \quad (\text{C7})$$

$$A_3 = \frac{(1-\gamma)(\nu-1)^2(\nu+1)(\gamma-\nu)((\nu+1)(b(\nu-1)(\gamma+\nu) + 2c_1\nu)^2 + 4(1-\gamma)\gamma\nu(1-\nu)^2 + 4(-d_1)\nu^2)}{2\nu^2(\gamma+\nu)} > 0. \quad (\text{C8})$$

- (3) Proof of (d) $\partial_y^2 H(y,x) < 0$ for $(x,y) \in [-1, 1] \times [-1/\nu, -1]$

$\partial_y^2 H(y,x) < 0$ is obvious by writing it as

$$\partial_y^2 H(y,x) = -B_1(1+x)^2 - B_2(1-x)^2 - B_3(1-x^2), \quad (\text{C9})$$

where

$$B_1 = 2(1-\gamma)c_1^2 c_3 \nu (1+\nu) > 0,$$

$$B_2 = (1-\gamma)(1-\nu)^2 (2\nu c_1 + (\gamma-\nu)(1-\nu)b)^2 > 0,$$

$$B_3 = (1-\gamma)(1-\nu)[4c_1^2 \nu^2 (2-\gamma+\nu) + 4bc_1(\gamma-\nu)\nu(1-\nu^2) + (1-\nu)^3(\gamma^2 - \nu^2)b^2] > 0. \quad (\text{C10})$$

- (4) Proof of (e) $\partial_y H(y=-1, x) + H(y=-1, x) > 0$ for $x \in [-1, 1]$

$\partial_y H(y=-1, x) + H(y=-1, x) > 0$ becomes obvious by writing it as

$$\partial_y H(y=-1, x) + H(y=-1, x) = C_1(1+x)^2 + C_2(1-x)^2 + C_3(1-x^2), \quad (\text{C11})$$

where

$$\begin{aligned} C_1 &= -c_1^2(\nu+1)(1-\nu^2)(2(1-\gamma)^2 - b^2(\gamma^2 - \nu^2)) + 2bc_1(\gamma-1)(\nu^2-1)^2(\gamma-\nu) + (1-\gamma)^2(\nu-1)^4(2-\gamma+\nu), \\ C_2 &= 2bc_1(\gamma-1)(\nu^2-1)(\nu-1)^2(\gamma-\nu) - 2c_1^2(\gamma-1)(\nu+1)(\nu-1)^3 + (1-\gamma)^2(\nu-1)^4(2-\gamma+\nu), \\ C_3 &= 2(1-\gamma)(-d_1)(\nu-1)^2(2-\gamma+\nu) > 0. \end{aligned} \quad (C12)$$

To see $C_1 > 0$ and $C_2 > 0$, one can write them by using Eq. (114) as

$$C_1 = \frac{a(2-a)(1-\nu)^4(1-\gamma)^3}{b^2(1-a)^2(1+a)^2} \left[-\frac{2b(1+b)^2(1-a+a^2)(1-a)^2\nu}{1-\nu} + (2-a)a(-b(1-a+a^2) + ab^2(2-a)) \right] > 0, \quad (C13)$$

and

$$C_2 = \frac{(1-\gamma)^3(1-\nu)^4}{b^2} \left[\frac{(1-a+a^2)^2(1+b)^2}{1-a^2} + ab^2(2-a)(1+2a-2a^2) - \frac{2b(1-a+a^2)(1+a(1-a)^2)}{1-a} \right] > 0. \quad (C14)$$

-
- [1] R. Emparan and H. S. Reall, Black holes in higher dimensions, *Living Rev. Relativity* **11**, 6 (2008).
- [2] R. Emparan and H. S. Reall, Black rings, *Classical Quantum Gravity* **23**, R169 (2006).
- [3] S. Mizoguchi and N. Ohta, More on the similarity between $D = 5$ simple supergravity and M theory, *Phys. Lett. B* **441**, 123 (1998).
- [4] S. Mizoguchi and G. Schroder, On discrete U duality in M theory, *Classical Quantum Gravity* **17**, 835 (2000).
- [5] E. Cremmer, B. Julia, H. Lu, and C. N. Pope, Dualization of dualities. 1., *Nucl. Phys.* **B523**, 73 (1998).
- [6] E. Cremmer, B. Julia, H. Lu, and C. N. Pope, Dualization of dualities. 2. Twisted self-duality of doubled fields, and superdualities, *Nucl. Phys.* **B535**, 242 (1998).
- [7] J. Ford, S. Giusto, A. Peet, and A. Saxena, Reduction without reduction: Adding KK-monopoles to five dimensional stationary axisymmetric solutions, *Classical Quantum Gravity* **25**, 075014 (2008).
- [8] D. V. Gal'tsov and N. G. Scherbluk, Hidden symmetries in 5D supergravities and black rings, *Proc. Sci., BHGRS2008* (2008) 016 [arXiv:0912.2770].
- [9] D. V. Gal'tsov and N. G. Scherbluk, Generating technique for $U(1)^*3$ 5D supergravity, *Phys. Rev. D* **78**, 064033 (2008).
- [10] D. V. Gal'tsov and N. G. Scherbluk, Improved generating technique for $D = 5$ supergravities and squashed Kaluza-Klein black holes, *Phys. Rev. D* **79**, 064020 (2009).
- [11] G. Compere, S. de Buyl, E. Jamsin, and A. Virmani, G_2 dualities in $D = 5$ supergravity and black strings, *Classical Quantum Gravity* **26**, 125016 (2009).
- [12] P. Figueras, E. Jamsin, J. V. Rocha, and A. Virmani, Integrability of five dimensional minimal supergravity and charged rotating black holes, *Classical Quantum Gravity* **27**, 135011 (2010).
- [13] S. Mizoguchi and S. Tomizawa, New approach to solution generation using $SL(2, R)$ duality of a dimensionally reduced space in five-dimensional minimal supergravity and new black holes, *Phys. Rev. D* **84**, 104009 (2011).
- [14] A. Bouchareb, G. Clement, C. M. Chen, D. V. Gal'tsov, N. G. Scherbluk, and T. Wolf, G_2 generating technique for minimal $D = 5$ supergravity and black rings, *Phys. Rev. D* **76**, 104032 (2007); *Phys. Rev. D* **78**, 029901(E) (2008).
- [15] R. C. Myers and M. J. Perry, Black holes in higher dimensional space-times, *Ann. Phys. (N.Y.)* **172**, 304 (1986).
- [16] R. Emparan and H. S. Reall, A rotating black ring solution in five-dimensions, *Phys. Rev. Lett.* **88**, 101101 (2002).
- [17] S. Hollands and S. Yazadjiev, Uniqueness theorem for 5-dimensional black holes with two axial Killing fields, *Commun. Math. Phys.* **283**, 749 (2008).
- [18] T. Mishima and H. Iguchi, New axisymmetric stationary solutions of five-dimensional vacuum Einstein equations with asymptotic flatness, *Phys. Rev. D* **73**, 044030 (2006).
- [19] P. Figueras, A black ring with a rotating 2-sphere, *J. High Energy Phys.* **07** (2005) 039.
- [20] A. A. Pomeransky and R. A. Sen'kov, Black ring with two angular momenta, arXiv:hep-th/0612005.
- [21] J. Evslin, Geometric engineering 5d black holes with rod diagrams, *J. High Energy Phys.* **09** (2008) 004.
- [22] Y. Chen and E. Teo, A rotating black lens solution in five dimensions, *Phys. Rev. D* **78**, 064062 (2008).
- [23] S. Tomizawa and T. Mishima, Stationary and biaxisymmetric four-soliton solution in five dimensions, *Phys. Rev. D* **99**, 104053 (2019).
- [24] J. Lucietti and F. Tomlinson, On the nonexistence of a vacuum black lens, *J. High Energy Phys.* **02** (2020) 005.
- [25] J. P. Gauntlett, J. B. Gutowski, C. M. Hull, S. Pakis, and H. S. Reall, All supersymmetric solutions of minimal

- supergravity in five- dimensions, *Classical Quantum Gravity* **20**, 4587 (2003).
- [26] H. S. Reall, Higher dimensional black holes and supersymmetry, *Phys. Rev. D* **68**, 024024 (2003); *Phys. Rev. D* **70**, 089902(E) (2004).
- [27] J. C. Breckenridge, R. C. Myers, A. W. Peet, and C. Vafa, D-branes and spinning black holes, *Phys. Lett. B* **391**, 93 (1997).
- [28] H. Elvang, R. Emparan, D. Mateos, and H. S. Reall, A supersymmetric black ring, *Phys. Rev. Lett.* **93**, 211302 (2004).
- [29] H. K. Kunduri and J. Lucietti, Supersymmetric black holes with lens-space topology, *Phys. Rev. Lett.* **113**, 211101 (2014).
- [30] S. Tomizawa and M. Nozawa, Supersymmetric black lenses in five dimensions, *Phys. Rev. D* **94**, 044037 (2016).
- [31] V. Breunhölder and J. Lucietti, Moduli space of supersymmetric solitons and black holes in five dimensions, *Commun. Math. Phys.* **365**, 471 (2019).
- [32] S. Tomizawa, Y. Yasui, and A. Ishibashi, Uniqueness theorem for charged rotating black holes in five-dimensional minimal supergravity, *Phys. Rev. D* **79**, 124023 (2009).
- [33] M. Cvetič and D. Youm, General rotating five-dimensional black holes of toroidally compactified heterotic string, *Nucl. Phys.* **B476**, 118 (1996).
- [34] J. L. Friedman, K. Schleich, and D. M. Witt, Topological censorship, *Phys. Rev. Lett.* **71**, 1486 (1993); *Phys. Rev. Lett.* **75**, 1872(E) (1995).
- [35] S. Hollands, J. Holland, and A. Ishibashi, Further restrictions on the topology of stationary black holes in five dimensions, *Ann. Henri Poincaré* **12**, 279 (2011).
- [36] G. W. Gibbons, D. Ida, and T. Shiromizu, Uniqueness and nonuniqueness of static vacuum black holes in higher dimensions, *Prog. Theor. Phys. Suppl.* **148**, 284 (2003).
- [37] G. W. Gibbons, D. Ida, and T. Shiromizu, Uniqueness of (dilaton) charged black holes and black p-branes in higher dimensions, *Phys. Rev. D* **66**, 044010 (2002).
- [38] F. R. Tangherlini, Schwarzschild field in n dimensions and the dimensionality of space problem, *Nuovo Cimento* **27**, 636 (1963).
- [39] H. K. Kunduri and J. Lucietti, Black hole non-uniqueness via spacetime topology in five dimensions, *J. High Energy Phys.* **10** (2014) 082.
- [40] J. Ehlers, Dissertation, Hamburg University.
- [41] B. K. Harrison, New solutions of the Einstein-Maxwell equations from old, *J. Math. Phys. (N.Y.)* **9**, 1744 (1968).
- [42] H. Stephani, D. Kramer, M. A. H. MacCallum, C. Hoenselaers, and E. Herlt, *Exact Solutions of Einstein's Field Equations*, 2nd ed. (Cambridge University Press, Cambridge, England, 2003).
- [43] A. H. Chamseddine and H. Nicolai, Coupling the SO(2) supergravity through dimensional reduction, *Phys. Lett.* **96B**, 89 (1980); *Phys. Lett.* **785B**, 631(E) (2018).
- [44] E. Cremmer and B. Julia, The SO(8) supergravity, *Nucl. Phys.* **B159**, 141 (1979).
- [45] S. Mizoguchi and S. Tomizawa, Flipped $SL(2, R)$ duality in five-dimensional supergravity, *Phys. Rev. D* **86**, 024022 (2012).
- [46] S. Tomizawa and S. Mizoguchi, General Kaluza-Klein black holes with all six independent charges in five-dimensional minimal supergravity, *Phys. Rev. D* **87**, 024027 (2013).
- [47] S. Tomizawa, Y. Yasui, and Y. Morisawa, Charged rotating Kaluza-Klein black holes generated by G2(2) transformation, *Classical Quantum Gravity* **26**, 145006 (2009).
- [48] D. Rasheed, The rotating dyonic black holes of Kaluza-Klein theory, *Nucl. Phys.* **B454**, 379 (1995).
- [49] H. Ishihara and K. Matsuno, Kaluza-Klein black holes with squashed horizons, *Prog. Theor. Phys.* **116**, 417 (2006).
- [50] R. Suzuki and S. Tomizawa, New construction of a charged dipole black ring by Harrison transformation, *Phys. Rev. D* **109**, 084020 (2024).
- [51] V. A. Belinsky and V. E. Sakharov, Stationary gravitational solitons with axial symmetry, *Sov. Phys. JETP* **50**, 1 (1979).
- [52] V. A. Belinski and E. Verdaguer, *Gravitational Solitons*, (Cambridge University Press, Cambridge, England, 2001).
- [53] A. A. Pomeransky, Complete integrability of higher-dimensional Einstein equations with additional symmetry, and rotating black holes, *Phys. Rev. D* **73**, 044004 (2006).
- [54] R. Emparan and H. S. Reall, Generalized Weyl solutions, *Phys. Rev. D* **65**, 084025 (2002).
- [55] T. Harmark, Stationary and axisymmetric solutions of higher-dimensional general relativity, *Phys. Rev. D* **70**, 124002 (2004).
- [56] H. Iguchi and T. Mishima, Solitonic generation of five-dimensional black ring solution, *Phys. Rev. D* **73**, 121501 (2006).
- [57] S. Tomizawa and M. Nozawa, Vacuum solutions of five-dimensional Einstein equations generated by inverse scattering method. II. Production of black ring solution, *Phys. Rev. D* **73**, 124034 (2006).
- [58] S. Tomizawa, Y. Morisawa, and Y. Yasui, Vacuum solutions of five dimensional Einstein equations generated by inverse scattering method, *Phys. Rev. D* **73**, 064009 (2006).
- [59] S. Tomizawa, H. Iguchi, and T. Mishima, Relationship between solitonic solutions of five-dimensional Einstein equations, *Phys. Rev. D* **74**, 104004 (2006).
- [60] H. Elvang and P. Figueras, Black saturn, *J. High Energy Phys.* **05** (2007) 050.
- [61] K. Izumi, Orthogonal black di-ring solution, *Prog. Theor. Phys.* **119**, 757 (2008).
- [62] H. Elvang and M. J. Rodriguez, Bicycling black rings, *J. High Energy Phys.* **04** (2008) 045.
- [63] H. Iguchi and T. Mishima, Black di-ring and infinite nonuniqueness, *Phys. Rev. D* **75**, 064018 (2007); *Phys. Rev. D* **78**, 069903(E) (2008).
- [64] J. Evslin and C. Krishnan, The black di-ring: An inverse scattering construction, *Classical Quantum Gravity* **26**, 125018 (2009).
- [65] S. Tomizawa, H. Iguchi, and T. Mishima, Rotating black holes on Kaluza-Klein bubbles, *Phys. Rev. D* **78**, 084001 (2008).
- [66] H. Iguchi, T. Mishima, and S. Tomizawa, Boosted black holes on Kaluza-Klein bubbles, *Phys. Rev. D* **76**, 124019 (2007); *Phys. Rev. D* **78**, 109903(E) (2008).
- [67] Y. Morisawa, S. Tomizawa, and Y. Yasui, Boundary value problem for black rings, *Phys. Rev. D* **77**, 064019 (2008).
- [68] Y. Chen and E. Teo, Black holes on gravitational instantons, *Nucl. Phys.* **B850**, 253 (2011).

- [69] Y. Chen, K. Hong, and E. Teo, Unbalanced Pomeransky-Sen'kov black ring, *Phys. Rev. D* **84**, 084030 (2011).
- [70] H. Iguchi, K. Izumi, and T. Mishima, Systematic solution-generation of five-dimensional black holes, *Prog. Theor. Phys. Suppl.* **189**, 93 (2011).
- [71] J. V. Rocha, M. J. Rodriguez, and A. Virmani, Inverse scattering construction of a dipole black ring, *J. High Energy Phys.* **11** (2011) 008.
- [72] Y. Chen, K. Hong, and E. Teo, A doubly rotating black ring with dipole charge, *J. High Energy Phys.* **06** (2012) 148.
- [73] Y. Chen and E. Teo, Rotating black rings on Taub-NUT, *J. High Energy Phys.* **06** (2012) 068.
- [74] J. V. Rocha, M. J. Rodriguez, and O. Varela, An electrically charged doubly spinning dipole black ring, *J. High Energy Phys.* **12** (2012) 121.
- [75] A. Feldman and A. A. Pomeransky, Charged black rings in supergravity with a single non-zero gauge field, *J. High Energy Phys.* **07** (2012) 141.
- [76] Y. Chen, Gravitational multisoliton solutions on flat space, *Phys. Rev. D* **93**, 044021 (2016).
- [77] J. Lucietti and F. Tomlinson, Moduli space of stationary vacuum black holes from integrability, *Adv. Theor. Math. Phys.* **26**, 371 (2022).
- [78] S. Tomizawa and R. Suzuki, Black lens in a bubble of nothing, *Phys. Rev. D* **106**, 124029 (2022).
- [79] R. Suzuki and S. Tomizawa, Capped black hole in five dimensions, *Phys. Rev. D* **109**, L121503.
- [80] C. W. Misner, The flatter regions of Newman, Unti and Tamburino's generalized Schwarzschild space, *J. Math. Phys.* **4**, 924 (1963).
- [81] H. K. Kunduri and J. Lucietti, The first law of soliton and black hole mechanics in five dimensions, *Classical Quantum Gravity* **31**, 032001 (2014).
- [82] M. Cvetič and D. Youm, Entropy of nonextreme charged rotating black holes in string theory, *Phys. Rev. D* **54**, 2612 (1996).
- [83] P. Orlik and F. Raymond, Actions of the Torus on 4-Manifolds. I, *Trans. Am. Math. Soc.* **152**, 531 (1970).
- [84] F. Tomlinson, Five-dimensional electrostatic black holes in a background field, *Classical Quantum Gravity* **39**, 135008 (2022).